Chapter 4[1]
Lateral Loads

1. Description of the Problem

a. Design philosophy. Deep foundations must often support substantial lateral loads as well as axial loads. While axially loaded, deep foundation elements may be adequately designed by simple statis methods, design methodology for lateral loads is more complex. The solution must ensure that equilibrium and soil-structure-interation compatability are satisfied. Nonlinear soil response complicates the solution. Batter piles are included in pile groups to improve the lateral capacity when vertical piles alone are not sufficient to support the loads.

b. Cause of lateral loads. Some causes of lateral loads are wind forces on towers, buildings, bridges and large signs, the centripetal force from vehicular traffic on curved highway bridges, force of water flowing against the substructure of bridges, lateral seismic forces from earthquakes, and backfill loads behind walls.

c. Factors influencing behavior. The behavior of laterally loaded deep foundations depends on stiffness of the pile and soil, mobilization of resistance in the surrounding soil, boundary conditions (fixity at ends of deep foundation elements), and duration and frequency of loading.

2. Nonlinear Pile and *p-y* Model for Soil.

a. General concept. The model shown in Figure 4-1 is emphasized in this document. The loading on the pile is general for the two-dimensional case (no torsion or out-of-plane bending). The horizontal lines across the pile are intended to show that it is made up of different sections; for example, steel pipe could be used with the wall thickness varied along the length. The difference-equation method is employed for the solution of the beam-column equation to allow the different values of bending stiffness to be addressed. Also, it is possible, but not frequently necessary, to vary the bending stiffness with bending moment that is computed during interation

b. Axial load. An axial load is indicated and is considered in the solution with respect to its effect on bending and not in regard to computing the required length to support a given axial load. As shown later, the computational procedure allows the detrmination of the axial load at which the pile will buckle.

c. Soil representation. The soil around the pile is replaced by a set of mechanisms indicating that the soil resistance p is a nonlinear function of pile deflection y. The mechanisms, and the corresponding curves that represent their behavior, are widely spaced but are considered to be very close in the analysis. As may be seen in Figure 4-1, the *p-y* curves are fully nonlinear with respect to distance x along the pile and pile deflection y. The curve for $x = x_1$ is drawn to indicate that the pile may deflect a finite distance with no soil resistance. The curve at $x = x_2$ is drawn to show that the soil is deflection-softening. There is no reasonable limit to the variations that can be employed in representing the response of the soil to the lateral deflection of a pile.

d. The p-y curve method. The *p-y* method is extremely versatile and provides a practical means for design. The method was suggested over 30 years ago (McCelland and Focht 1958). Two developments during the 1950's made the method possible: the digital computer for solving the problem of the nonlinear, fourth-order differential equation for the beam-column; and the remote-reading strain gauge for use in obtaining soil-response (*p-y*) curves from field experiments. The method has been used by the petroleum industry in the design of pile-supported platforms and extended to the design of onshore foundations as, for example by publications of the Federal Highway Administration (USA) (Reese 1984).

(1) Definition of p and y. The definition of the quantities p and y as used here is necessary because other approaches have been used. The sketch in Figure 4-2a shows a uniform distribution of unit stresses normal to the wall of a cylindrical pile. This distribution is correct for the case of a pile that has been installed without bending. If the pile is caused to deflect a distance y (exaggerated in the sketch for clarity), the distribution of unit stresses would be similar to that shown in Figure 4-2b. The stresses would have decreased on the back side of the pile and increased on the front side. Both normal and a shearing stress component may developed along the perimeter of the cross section. Integration of the unit stresses will result in the quanity p which acts opposite in direction to y. The dimensions of p are load per unit length along the pile. The definitions of p and y that are presented are convenient in the solution of the differential equation and are consistent with the quantities used in the solution of the ordinary beam equation.

(2) Nature of soil response. The manner in which the soil responds to the lateral deflection of a pile can be examined by examined by considering the pipe pile shown

[1]Portions of this chapter were abstracted from the writings of Dr. L. C. Reese and his colleagues, with the permission of Dr. Reese.

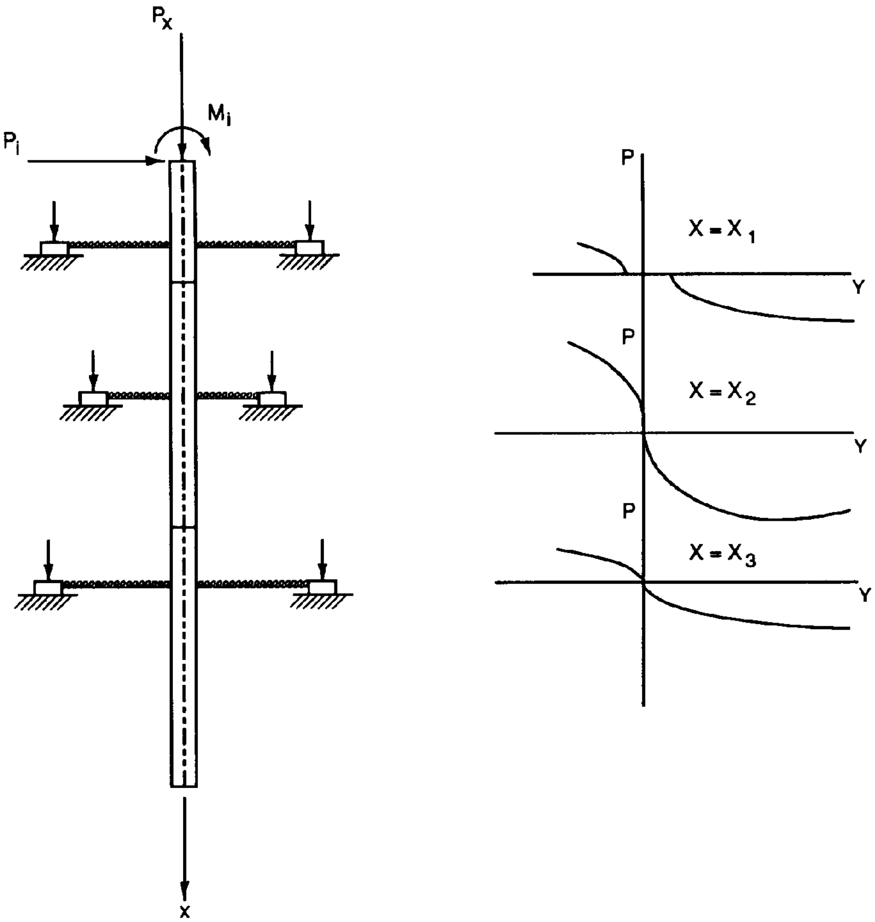

Figure 4-1. Model of pile under lateral loading with *p-y* curves

in Figure 4-3. Two slices of soil are indicated; the element *A* is near the ground surface and the element *B* is several diameters below the ground surface. Consideration will be given here to the manner in which those two elements of soil react as the pile deflects under an applied lateral load. Figure 4-4 shows a *p-y* curve that is conceptual in nature. The curve is plotted in the first quadrant for convenience and only one branch is shown. The curve properly belongs in the second and fourth quadrants because the soil response acts in opposition to the deflection. The branch of the *p-y* curves 0-a is representative of the elastic action of the soil; the deflection at point *a* may be small. The branch *a-b* is the transition portion of the curve. At point *b* the ultimate soil resistance is reached. The following paragraphs will deal with the ultimate soil resistance.

(a) Ultimate resistance to lateral movement. With regard to the ultimate resistance at element *A* in Figure 4-3, Figure 4-5 shows a wedge of soil that is moved up and away from a pile. The ground surface is represented by the plane ABCD, and soil in contact with the pile is represented by the surface CDEF. If the pile is moved in the direction indicated, failure of the soil in shear will occur on the planes ADE, BCF, and AEFB. The horizontal force F_p against the pile can be computed by summing the horizontal components of the forces on the sliding surfaces, taking into account ote gravity force on the wedge of soil. For a given value of *H*, it is assumed that the value of the horizontal force on the pile is

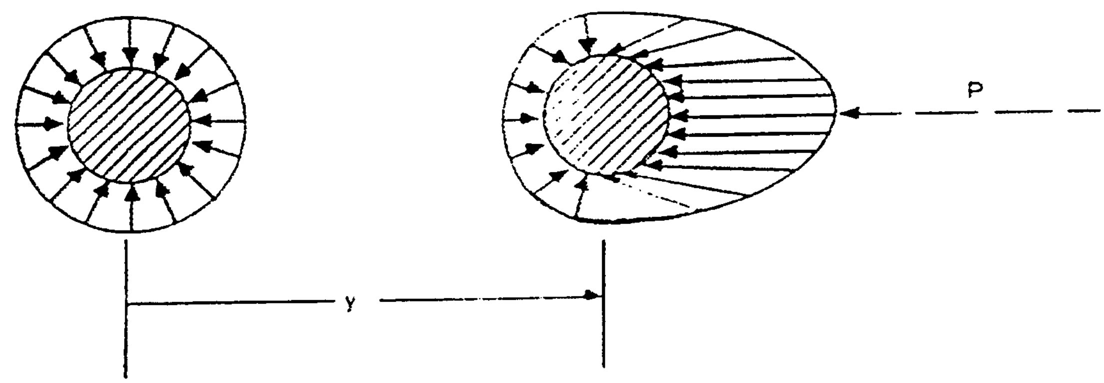

(a) Before bending (b) After bending

Figure 4-2. Distribution of unit stresses against a pile before and after lateral deflection

F_{p1}. If a second computation is made with the depth of the wedge increased by ΔH, the horizontal force will be F_{p2}. The value of p_u for the depth z where z is equal approximately to $(2H + \Delta H)/2$ can be computed: $(p_u)_z = (F_{p2} - F_{p1})/\Delta H$.

(b) Resistance at ground level. At the ground surface, the value of p_u for sand must be zero because the weight of the wedge is zero and the forces on the sliding surfaces will be zero. At the ground surface for clay, on the other hand, the values of p_u will be larger than zero because the cohesion of the clay, which is independent of the overburden stress, will generate a horizontal force.

(c) Resistance below ground level. A plan view of a pile at several diameters below the ground surface,corresponding to the element at B in Figure 4-3, is shown in Figure 4-6. The potential failure surfaces that are shown are indicative of plane-strain failure; while the ultimate resistance p_u cannot be determined precisely, elementary concepts can be used to develop approximate expressions.

(3) Effects of loading . As will be shown in detail in the next sections, the soil response can be affected by the way the load is applied to a pile. Recommendations are given herein for the cases where the load is short-term (static) or is repeated (cyclic). The latter case is frequently encountered in design. Loadings that are sustained or dynamic (due to machinery or a seismic event) are special cases; the methods of dealing with these types of loading are not well developed and are not addressed herein. The cyclic loading of sands also causes a reduced resistance in sands, but the reduction is much less severe than experienced by clays.

(4) Presence of water. The presence of water will affect the unit weight of the soil and will perhaps affect other properties to some extent; however, water above the ground surface has a pronounced effect on the response of clay soils, particularly stiff clay. Cyclic loading has two types of deleterious effects on clays; there is likely to be (1) strain softening due to repeated deformations and (2) scour at the pile-soil interface. This latter effect can be the most serious. If the deflection of the pile is greater that at point a in Figure 4-4 or certainly if the deflection is greater than that at point b, a space will open as the load is released. The space will fill with water and the water will be pushed upward, or through cracks in the clay, with the next cycle of loading. The velocity of the water cxan be such that considerable quantities of soil are washed ot the ground surface, causing a significant loss in soil resistance.

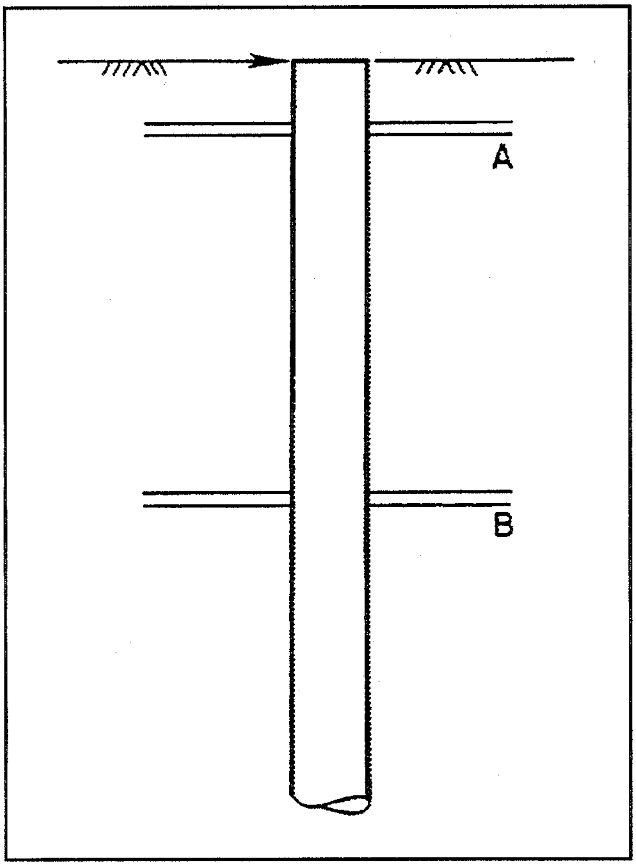

Figure 4-3. Pipe pile and soil elements

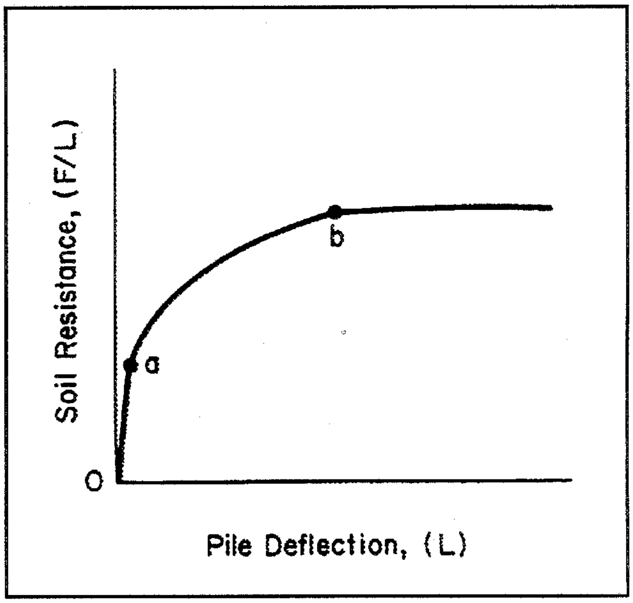

Figure 4-4. Conceptual *p-y* curve

3. Development of *p-y* Curve for Soils

Detailed methods for obtaining *p-y* curves are presented in the following paragraphs. Recommendations are given for clay and sand, for static and cyclic loading, and for cases where the water table is above or below the ground surface. As will be seen, the soil properties that are needed for clay refer to undrained shear strength; there are no provisions for dealing with soils having both *c* and ϕ parameters.

a. p-y curves for soft clay. As noted earlier, there is a significant influence of the presence of water above the ground surface. If soft clay exists at the ground surface, it is obvious that water must be present at or above the ground surface or the clay would have become desiccated and stronger. If soft clay does not exist at the ground surface but exists at some distance below the ground surface, the deleterious effect of water moving in and out of a gap at the interface of the pile and soil will not occur; therefore, the *p-y* curves for clay above the ground surface should be used (Welch and Reese 1972). The *p-y* curves presented here are for soft clay, with water above the group surface, and the clay experienced the deteriorating effects noted earlier.

(1) Field experiments. Field experiments using full-sized, instrumented piles provide data from which *p-y* curves from static and cyclic loading can be generated. Such experimental curves are correlated with available theory to provide the basis to recommend procedures for developing *p-y* curves. Therefore, field experiments with instrumented piles are essential to the recommendations for *p-y* curves. Matlock (1970) performed lateral load tests employing a steel-pipe pile that was 12.75 inches in diameter and 42 feet long. It was driven into clays near Lake Austin that had a shear strength of about 800 pounds per square foot. The pile was recovered, taken to Sabine Pass, Texas, and driven into clay with a shear strength that averaged about 300 pounds per square foot in the significant upper zone. The studies carried out by Matlock led to the recommendations shown in the following paragraphs.

(2) Recommendations for computing *p-y* curves. The following procedure is for <u>short-term static loading</u> and is illustrated in Figure 4-7a.

(a) Obtain the best possible estimate of the variation with depth of undrained shear strength *c* and submerged unit weight γ'. Also obtain the values of ε_{50}, the strain corresponding to one-half the maximum principal-stress difference. If no stress-strain curves are available, typical values of ε_{50} are given in Table 4-1.

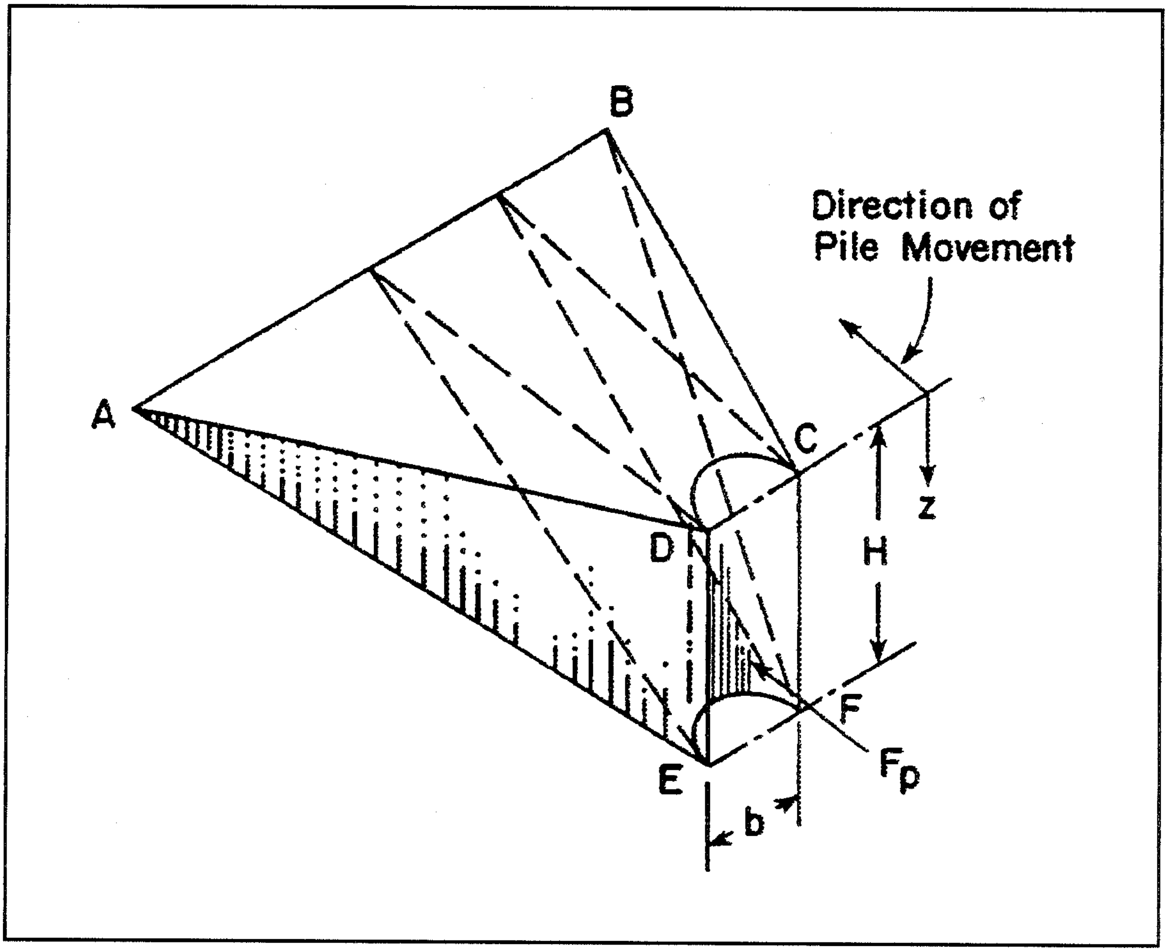

Figure 4-5. Wedge-type failure of surface soil

Table 4-1 Representative Values of ε_{50}	
Consistency of Clay	ε_{50}
Soft	0.020
Medium	0.010
Stiff	0.005

(b) Compute the ultimate soil resistance per unit length of pile, using the smaller of the values given by equations below

$$p_u = [3 + \frac{\gamma'}{c} \times + \frac{J}{b} \times]\ cb \qquad (4\text{-}1)$$

$$p_u = 9\ cb \qquad (4\text{-}2)$$

where

p_u = ultimate soil resistance

x = depth from ground surface to p-y curve

γ' = average effective unit weight from ground surface to depth x

c = shear strength at depth x

b = width of pile

J = empirical dimensionless parameter

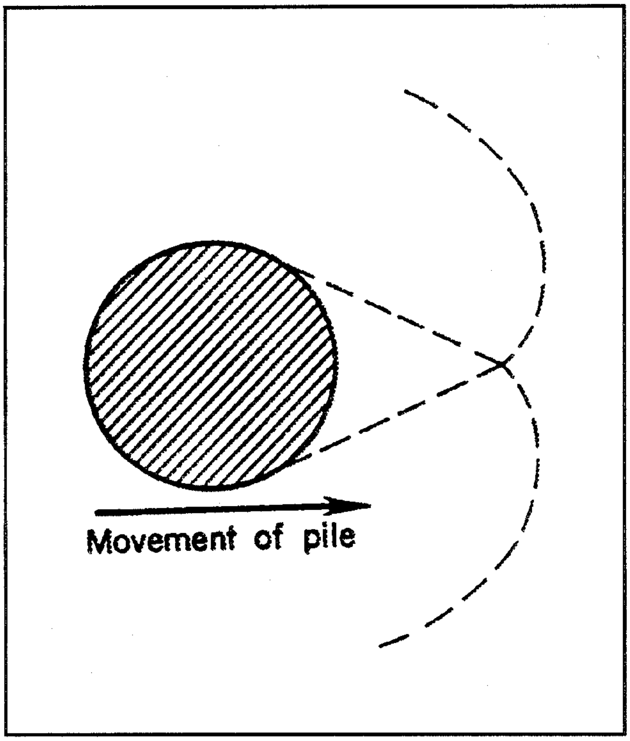

Figure 4-6. Potential failure surfaces generated by pile at several diameters below ground surface

Matlock (1970) stated that the value of J was determined experimentally to be 0.5 for a soft clay and about 0.25 for a medium clay. A value of 0.5 is frequently used for J. The value of p_u is computed at each depth where a p-y curve is desired, based on shear strength at that depth. A computer obtains values of y and the corresponding p-values at close spacings; if hand computations are being done, p-y curves should be computed at depths to reflect the soil profile. If the soil is homogeneous, the p-y curves should be obtained at close spacings near the ground surface where the pile deflection is greater.

(c) Compute the deflection, y_{50}, at one-half the ultimate soil resistance for the following equation:

$$y_{50} = 2.5\ \varepsilon_{50} b \qquad (4\text{-}3)$$

(d) Points describing the p-y curve are now computed from the following relationship.

$$\frac{p}{p_u} = 0.5\left(\frac{y}{y_{50}}\right) 0.333 \qquad (4\text{-}4)$$

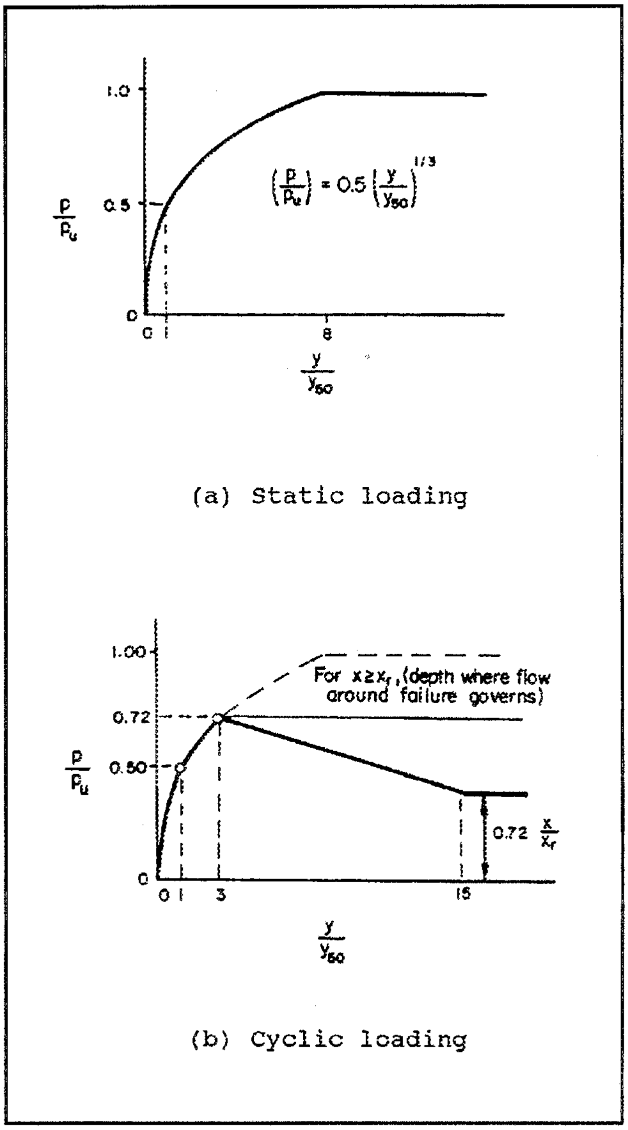

Figure 4-7. Characteristic shapes of the p-y curves for soft clay below the water table

The value of p remains constant beyond $y = 8y_{50}$.

(3) Procedure for cyclic loading. The following procedure is for cyclic loading and is illustrated in Figure 4-7b.

(a) Construct the p-y curve in the same manner as for short-term static loading for values of p less than $0.72p_u$.

(b) Solve equations 4-1 and 4-2 simultaneously to find the depth, x_r, where the transition occurs from the wedge-type failure to a flow-around failure. If the unit weight and shear strength are constant in the upper zone, then

$$x_r = \frac{6\ cb}{(\gamma' b + Jc)} \quad (4\text{-}5)$$

If the unit weight and shear strength vary with depth, the value of x_r should be computed with the soil properties at the depth where the p-y curve is desired.

(c) If the depth to the p-y curve is greater than or equal to x_r, then p is equal to $0.72p_u$ from $y = 3y_{50}$ to $y = 15y_{50}$.

(d) If the depth to the p-y curve is less than x_r, then the value of p decreases from $0.72p_u$ at $y = 3y_{50}$ to the value given by the following expression at $y = 15y_{50}$.

$$p = 0.72\ p_u (\frac{x}{x_r}) \quad (4\text{-}6)$$

The value of p remains constant beyond $y = 15y_{50}$.

(4) Recommended soil tests. For determining the values of shear strength of the various layers of soil for which p-y curves are to be constructed, Matlock (1970) recommended the following tests in order of preference:

(a) In situ vane-shear tests with parallel sampling for soil identification.

(b) Unconsolidated-undrained triaxial compression tests having a confining stress equal to the overburden pressure with c being defined as half the total maximum principal stress difference.

(c) Miniature vane tests of samples in tubes.

(d) Unconfined compression tests.

b. p-y curves for stiff clay below the water table.

(1) Field experiments. Reese, Cox, and Koop (1975) performed lateral load tests employing steel-pipe piles that were 24 inches in diameter and 50 feet long. The piles were driven into stiff clay as a site near Manor, TX. The clay had an undrained shear strength ranging from about 1 ton per square foot at the ground surface to about 3 tons per square foot at a depth of 12 feet. The studies that were carried out led to the recommendations shown in the following paragraphs.

(2) Recommendations for computing p-y curves. The following procedure is for short-term static loading and is illustrated by Figure 4-8. The empirical parameters, A_s and A_c shown in Figure 4-9 and k_s and k_c shown in Table 4-2 were determined from the results of the experiments.

(a) Obtain values for undrained soil shear strength c, soil submerged unit weight γ' and pile diameter b.

(b) Compute the average undrained soil shear strength c_a over the depth x.

(c) Compute the ultimate soil resistance per unit length of pile using the smaller of the values given by the equation below

$$p_{ct} = 2c_a b + \gamma' b x + 2.83\ c_a x \quad (4\text{-}7)$$

$$p_{cd} = 11\ cb \quad (4\text{-}8)$$

(d) Choose the appropriate values of the empirical parameter A_s from Figure 4-9 for the particular nondimensional depth.

(e) Establish the initial straight-line portion of the p-y curve:

$$p = (kx)y \quad (4\text{-}9)$$

Use the appropriate value of k_s or k_c from Table 4-2 for k.

(f) Compute the following:

$$y_{50} = \varepsilon_{50} b \quad (4\text{-}10)$$

Use an appropriate value of ε_{50} from results of laboratory tests or, in the absence of laboratory tests, from Table 4-3.

Table 4-2
Representative Values of *k* for Stiff Clays

	Average Undrained Shear Strength[1] ksf T/sq ft		
	1-2	**2-4**	**4-8**
k_s (Static) lb/cu in.	500	1,000	2,000
k_c (Static) lb/cu in.	200	400	800

[1] The average shear strength should be computed to a depth of five pile diameters. It should be defined as half the total maximum principal stress difference in an unconsolidated undrained triaxial test.

Table 4-3
Representative Values of ε_{50} for Stiff Clays

	Average Undrained Shear Strength ksf		
	1-2	2-4	4-8
ε_{50} (in./in.)	0.007	0.005	0.004

(g) Establish the first parabolic portion of the p-y curve, using the following equation and obtaining p_c from equations 4-7 or 4-8.

$$p = 0.5p_c\left(\frac{y}{y_{50}}\right)^{0.5} \qquad (4\text{-}11)$$

Equation 4-11 should define the portion of the p-y curve from the point of the intersection with equation 4-9 to a point where y is equal to $A_s y_{50}$ (see note in step j).

(h) Establish the second parabolic portion of the p-y curve,

$$p = 0.5p_c\left(\frac{y}{y_{50}}\right)^{0.5} - 0.555p_c\left(\frac{y - A_s y_{50}}{A_s y_{50}}\right)^{1.25} \qquad (4\text{-}12)$$

Equation 4-12 should define the portion of the p-y curve from the point where y is equal to $A y_{50}$ to a point where y is equal to $6A_s y_{50}$ (see note in step j).

(i) Establish the next straight-line portion of the p-y curve,

$$p = 0.5p_c(6A_s)^{0.5} - 0.411p_c - \left(\frac{0.0625}{y_{50}}\right) p_c\,(y - 6A_s y_{50}) \qquad (4\text{-}13)$$

Equation 4-13 should define the portion of the p-y curve from the point where y is equal to $6A_s y_{50}$ to a point where y is equal to $18A_y y_{50}$ (see note in step j).

(j) Establish the final straight-line portion of the curve,

$$p = 0.5p_c(6A_s)^{0.5} - 0.411p_c - 0.75p_c A_s \qquad (4\text{-}14)$$

or

$$p_c = p_c(1.225\sqrt{A_s} - 0.75A_s - 0.411) \qquad (4\text{-}15)$$

Equation 4-15 should define the portion of the p-y curve from the point where y is equal to $18A_s y_{50}$ and for all larger values of y (see following note).

Note: The step-by-step procedure is outlined, and Figure 4-8 is drawn, as if there is an intersection between equations 4-9 and 4-11. However, there may be no intersection of equation 4-9 with any of the other equations defining the p-y curve. If there is no intersection, the equation should be employed that gives the smallest value of p for any value of y.

(3) Procedure of cyclic loading. The following procedure is for cyclic loading and is illustrated in Figure 4-10.

(a) Step a is same as for static case.

(b) Step b is same as for static case.

(c) Step c is same as for static case.

(d) Choose the appropriate value of A_c from Figure 4-9 for the particular nondimensional depth.

Compute the following:

$$y_p = 4.1A_s y_{50} \qquad (4\text{-}16)$$

(e) Step e is same as for static case.

(f) Step f is same as for static case.

(g) Establish the parabolic portion of the p-y curve,

$$p = A_c p_c\left[1 - \left|\frac{y - 045y_p}{0.45y_p}\right|^{2.5}\right] \qquad (4\text{-}17)$$

Equation 4-17 should define the portion of the p-y curve from the point of the intersection with equation 4-9 to where y is equal to $0.6y_p$ (see note in step i).

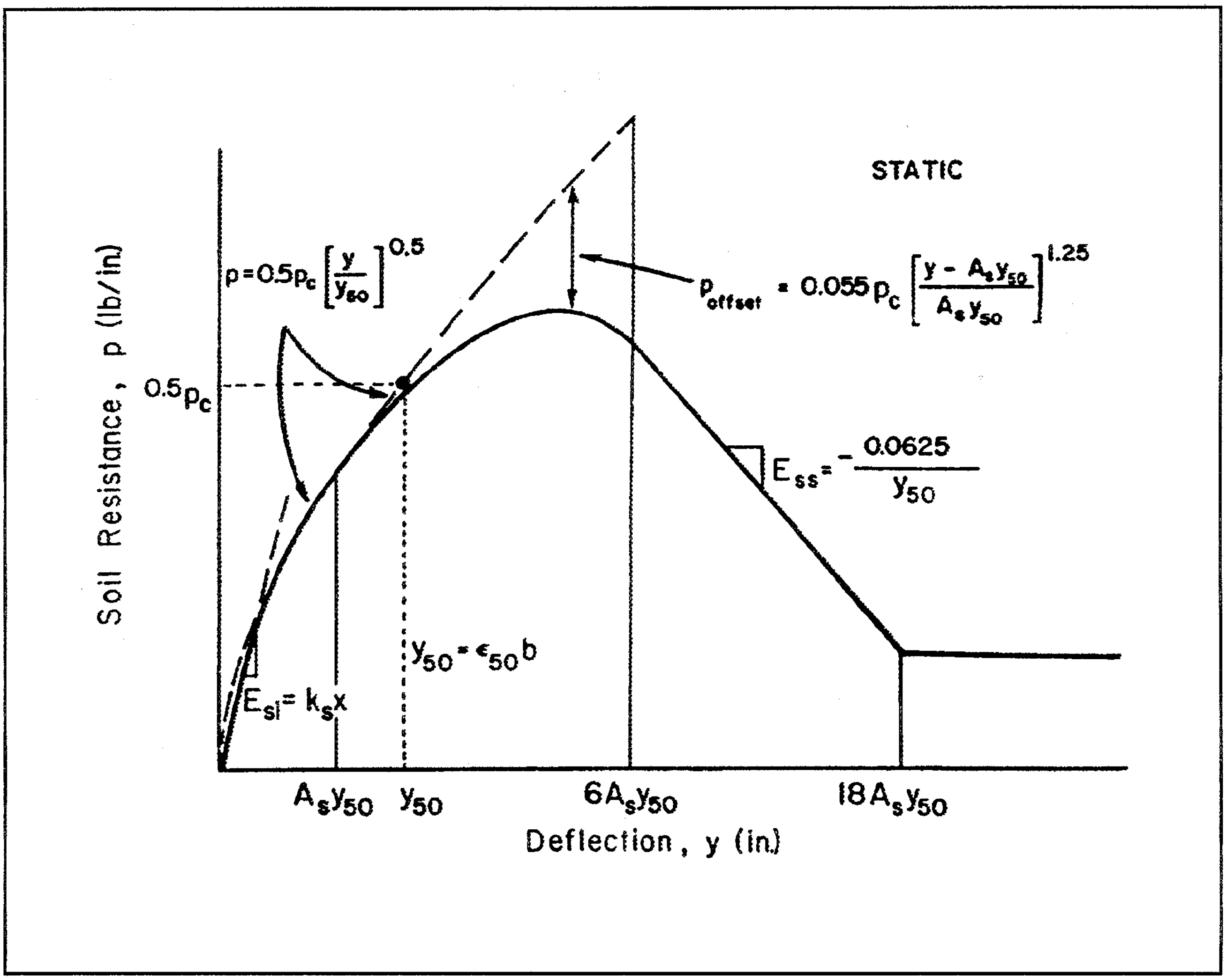

Figure 4-8. Charactertistic shape of *p-y* curve for static loading in stiff clay below the water table

(h) Establish the next straight-line portion of the *p-y* curve,

$$p = 0.936\,A_c p_c - \frac{0.085}{y_{50}}\,p_c(y - 0.6y_p) \qquad (4\text{-}18)$$

Equation 4-18 should define the portion of the *p-y* curve from the point where y is equal to $0.6y_p$ to the point where y is equal to $1.8y_p$ (see note in step h).

(i) Establish the final straight-line portion of the *p-y* curve,

$$p = 0.936\,A_c p_c - \frac{0.102}{y_{50}}\,p_c y_p \qquad (4\text{-}19)$$

Equation 4-19 should define the portion of the *p-y* curve from the point where y is equal to $1.8y_p$ and for all larger values of y (see following note).

Note: The step-by-step procedure is outlined, and Figure 4-10 is drawn, as if there is an intersection between equations 4-9 and 4-17. However, there may be no intersection of those two equations and there may be no intersection of equation 4-9 with any of the other equations defining the *p-y* curve. If there is no intersection, the equation should be employed that gives the smallest value of p for any value of y.

(4) Recommended soil tests. Triaxial compression tests of the unconsolidated-undrained type with confining pressures conforming to the in situ total overburden pressures are

illustrated in Figure 4-11.

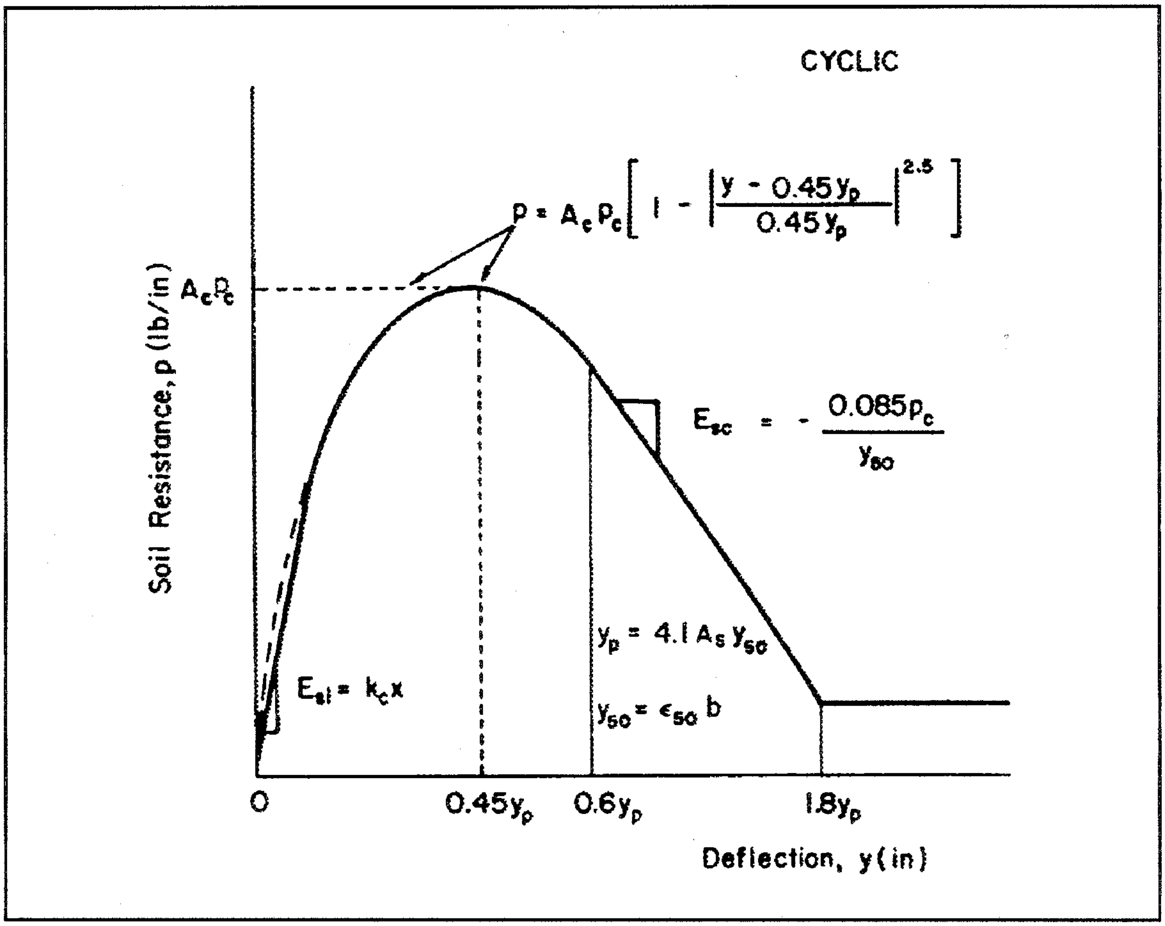

Figure 4-10. Characteristic shape of *p-y* curve for cyclic loading in stiff clay below the water table

ε_{50} from stress-strain curves. If no stress-strain curves are available, use a value from ε_{50} of 0.010 or 0.005 as given in Table 4-1, the larger value being more conservative.

(b) Compute the ultimate soil resistance per unit length of shaft, p_u, using the smaller of the values given by equations 4-1 and 4-2. (In the use of equation 4-1, the shear strength is taken as the average from the ground surface to the depth being considered and J is taken as 0.5. The unit weight of the soil should reflect the position of the water table.)

(c) Compute the deflection, y_{50} at one-half the ultimate soil resistance from equation 4-3.

(d) Points describing the p-y curve may be computed from the relationship below.

$$\frac{p}{p_u} = 0.5\left(\frac{y}{y_{50}}\right)^{0.25} \qquad (4\text{-}20)$$

(e) Beyond $y = 16y_{50}$, p is equal to p_u for all values of y.

(3) Procedure for cyclic loading. The following procedure is for cyclic loading and is illustrated in Figure 4-12.

(a) Determine the p-y curve for short-term static loading by the procedure previously given.

(b) Determine the number of times the design lateral load will be applied to the pile.

(c) For several values of p/p_u, obtain the value of C, the parameter describing the effect of repeated loading on deformation, from a relationship developed by laboratory tests

(Welch and Reese 1972), or in the absence of tests, from the following equation.

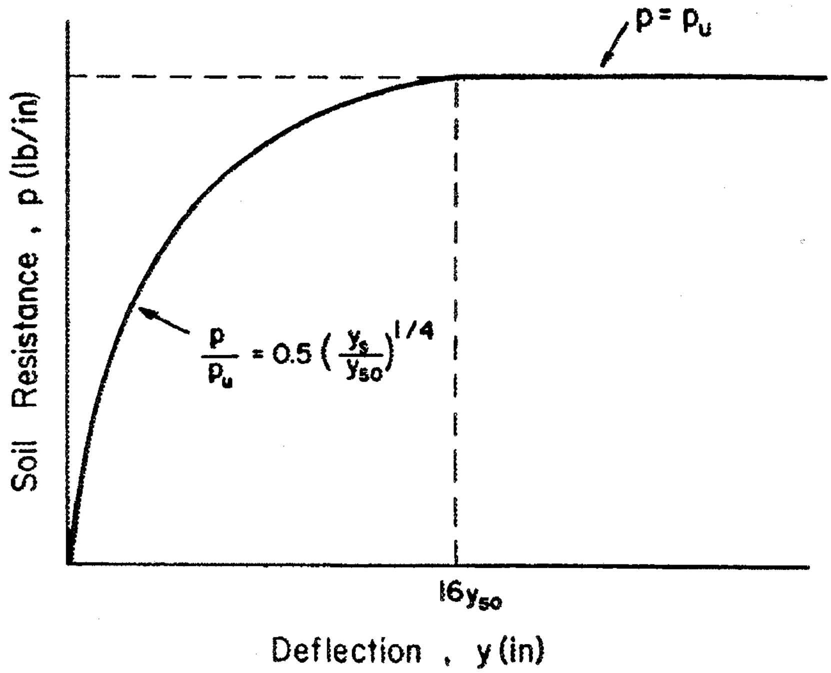

Figure 4-11. Characteristic shape of *p-y* curve for static loading in stiff clay above the water table

$$C = 9.6\left(\frac{p}{p_u}\right)^4 \qquad (4\text{-}21)$$

(d) At the value of p corresponding to the values of p/p_u selected in step c, compute new values of y for cyclic loading from the following equation.

$$y_c = y_s + y_{50} \times C \times \log N \qquad (4\text{-}22)$$

where

y_c = deflection under N-cycles of load

y_s = deflection under short-term static load

y_{50} = deflection under short-term static load at one-half the ultimate resistance

N = number of cycles of load application

(e) Define the soil response after N-cycles of load, using the *p-y* curve.

(4) Recommended soil tests. Triaxial compression tests of the unconsolidated-undrained type with confining stresses equal to the overburden pressures at the elevations from which the samples were taken are recommended to determine the shear strength. The value of ε_{50} should be taken as the strain during the test corresponding to the stress equal to half the maximum total principal stress difference. The undrained shear strength, *c*, should be defined as one-half the maximum total-principal-stress difference. The unit weight of the soil must also be determined.

d. p-y curves for sand. A major experimental program was conducted on the behavior of laterally loaded piles in sand below the water table. The results can be extended to sand above the water table by making appropriate adjustments in the values of the unit weight, depending on the position of the water table.

(1) Field experiments. An extensive series of tests were performed as a site on Mustang Island, near Corpus Christi

(Cox, Reese, and Grubbs 1974). Two steel-pipe piles, 24 inches in diameter, were driven into sand in a manner to simulate the driving of an open-ended pipe and were subjected to lateral oading. The embedded length of the piles was 69 feet. One of the piles was subjected to short-

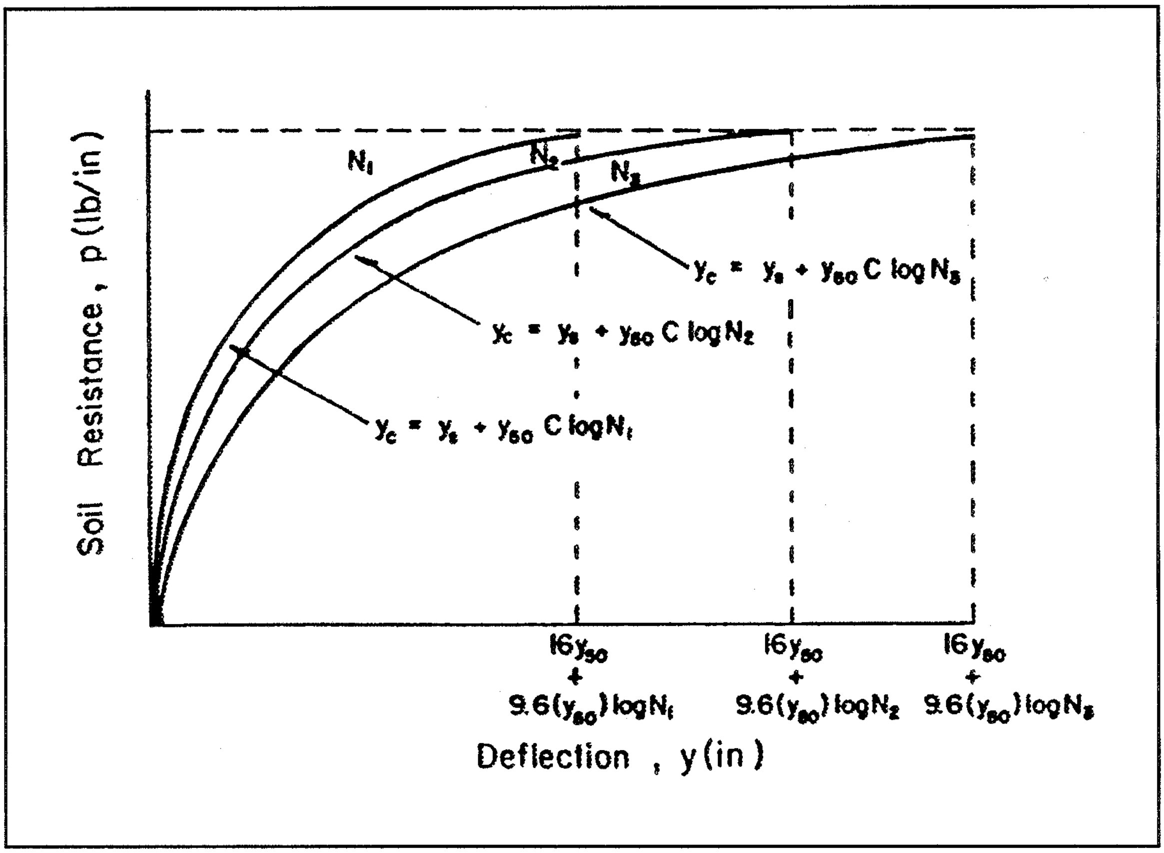

Figure 4-12. Characteristic shape of *p-y* curve for cyclic loading in stiff clay above the water table

term loading and the other to repeated loading. The soil at the site was a uniformly graded, fine sand with an angle of internal friction of 39 degrees. The submerged unit weight was 66 pounds per cubic foot. The water surface was maintained a few inches above the mudline throughout the test program.

(2) Recommendations for computing *p-y* curves. The following procedure is for short-term static loading and for cyclic loading and is illustrated in Figure 4-13 (Reese, Cox, and Koop 1974).

(a) Obtain values for the angle of internal friction ϕ, the soil unit weight γ, and pile diameter b.

(b) Make the following preliminary computations.

$$\alpha = \frac{\phi}{2};\ \beta = 45 + \frac{\phi}{2};\ K_o = 0.4;\ \text{and} \qquad (4\text{-}23)$$

$$K_a = \tan^2(45 - \frac{\phi}{2});\ K_p = \tan^2(45 - \frac{\phi}{2})$$

(c) Compute the ultimate soil resistance per unit length of pile using the smaller of the values given by the equations below, where x is equal to the depth below the ground surface.

$$p_{st} = \gamma b^2 \left[S_1 (\frac{x}{b}) + S_2 (\frac{x}{b})^2 \right] \qquad (4\text{-}24)$$

$$p_{sd} = \gamma b^2 [S_3 (\frac{x}{b})] \qquad (4\text{-}25)$$

where

$$S_1 = (K_p - K_a) \qquad (4\text{-}26)$$

$$S_2 = (\tan\beta)\,(K_{\tan}\alpha + K_o[\tan\phi \sin\beta\,(\sec\alpha + 1) - \tan\alpha]) \qquad (4\text{-}27)$$

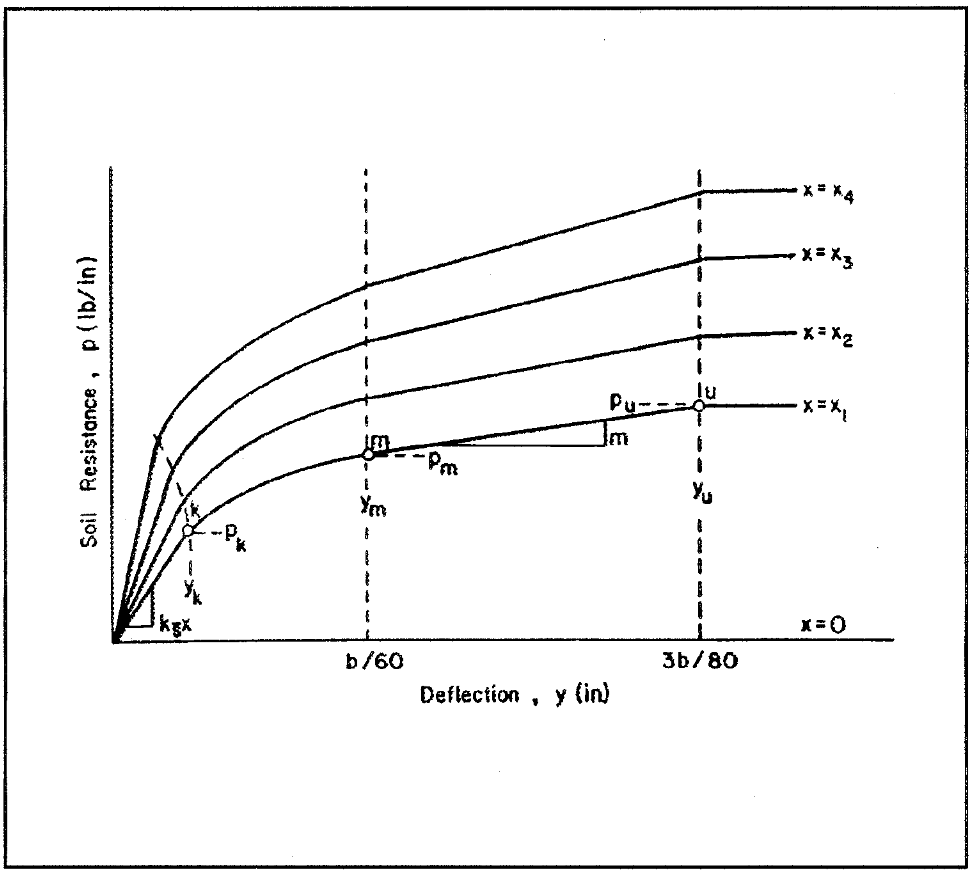

Figure 4-13. Characteristic shape of a family of *p-y* curves for static and cyclic loading in sand

$$S_3 = K^2 p (K_p + K_o \tan \phi) - K_a \tag{4-28}$$

(d) The depth of transition x_t can be found by equating the expressions in equations 4-24 and 4-25, as follows:

$$\frac{x_t}{b} = \frac{(S_3 - S_1)}{S_2} \tag{4-29}$$

The appropriate γ for the position of the water table should be employed. Use equation 39 above, x_t, and equation 40 below. It can be seen that S_1, S_2, S_3, x_t / b are functions only of ϕ; therefore, the values shown in Table 4-4 can be computed.

(e) Select a depth at which a *p-y* curve is desired.

(f) Establish y_u as 3b/80. Compute p_u by the following equation:

$$p_u = \overline{A}_s p_s \quad \text{or} \quad p_u = \overline{A}_c p_s \tag{4-30}$$

Use the appropriate value of $\overline{A}_s$ or $\overline{A}_c$ from Figure 4-14 for the particular nondimensional depth and for either the static or cyclic case. Use the appropriate equation for p_s, equation 4-24 or 4-25 by referring to the computation in step d.

(g) Establish y_m as b/60. Compute p_m by the following equation:

$$p_m = B_s p_s \quad \text{or} \quad p_m = B_c p_s \tag{4-31}$$

Use the appropriate value of B_s or B_c from Figure 4-15 for the particular nondimensional depth, and for either the static or cyclic case. Use the appropriate equation for p_s. The two

Table 4-4
Nondimensional Coefficients for *p-y* Curves for Sand

ϕ, deg	S_1	S_2	S_3	x_t/b
25.0	2.05805	1.21808	15.68459	11.18690
26.0	2.17061	1.33495	17.68745	11.62351
27.0	2.28742	1.46177	19.95332	12.08526
28.0	2.40879	1.59947	22.52060	12.57407
29.0	2.53509	1.74906	25.43390	13.09204
30.0	2.66667	1.91170	28.74513	13.64147
31.0	2.80394	2.08866	32.51489	14.22489
32.0	2.94733	2.28134	36.81400	14.84507
33.0	3.09733	2.49133	41.72552	15.50508
34.0	3.25442	2.72037	47.34702	16.20830
35.0	3.41918	2.97045	53.79347	16.95848
36.0	3.59222	3.24376	61.20067	17.75976
37.0	3.77421	3.54280	69.72952	18.61673
38.0	3.96586	3.87034	79.57113	19.53452
39.0	4.16799	4.22954	90.95327	20.51883
40.0	4.38147	4.62396	104.14818	21.56704

straight-line portions of the *p-y* curve, beyond the point where *y* is equal to b/60, can now be established.

(h) Establish the initial straight-line portion of the *p-y* curves,

$$p = (kx)y \tag{4-32}$$

Use Tables 4-4 and 4-5 to select an appropriate value of k.

(i) Establish the parabolic section of the *p-y* curve,

$$p = \overline{C}\, y^{1/n} \tag{4-33}$$

(3) Parabolic section. Fit the parabola between points *k* and *m* as follows:

(a) Get the slope of line between points *m* and *u* by,

$$m = \frac{p_u - p_m}{y_u - y_m} \tag{4-34}$$

(b) Obtain the power of the parabolic section by,

$$n = \frac{p_m}{m_{ym}} \tag{4-35}$$

(c) Obtain the coefficient $\overline{C}$ as follows:

$$\overline{C} = \frac{p_m}{y_m^{1/n}} \tag{4-36}$$

(d) Determine point *k* as

$$yk = \left(\frac{\overline{C}}{kx}\right)\ n/n-1 \tag{4-37}$$

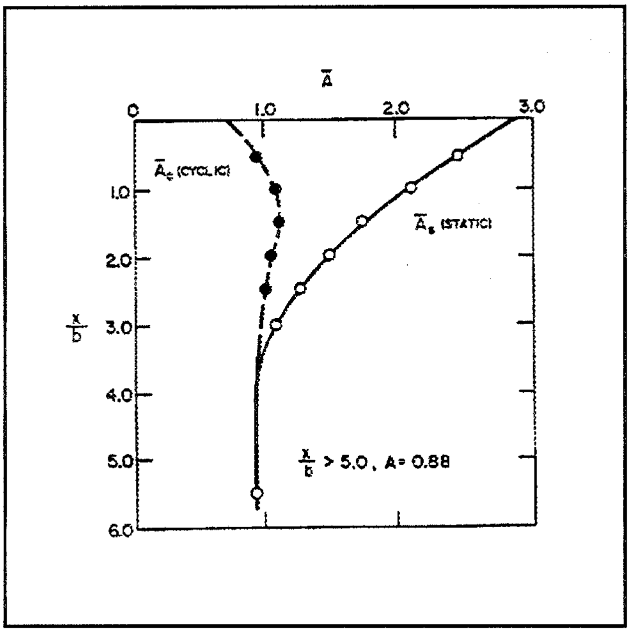

Figure 4-14. Values of coefficients $\overline{A_c}$ and $\overline{A_s}$

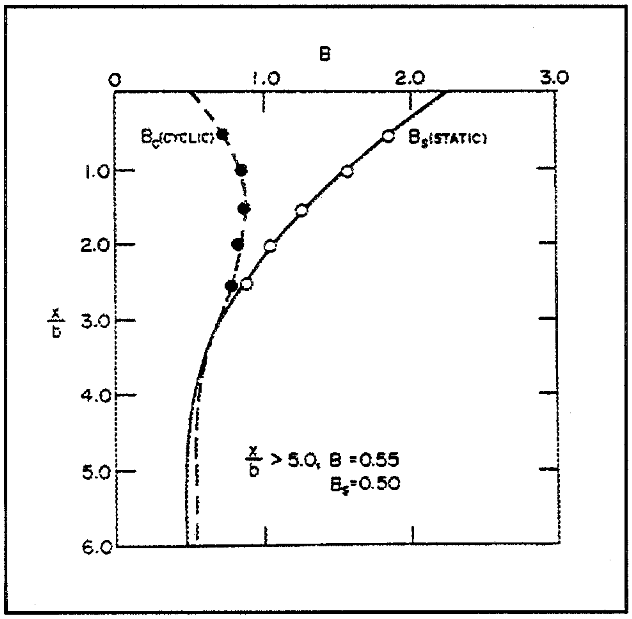

Figure 4-15. Nondimensional coefficient *B* for soil resistance versus depth

(e) Compute appropriate number of points on the parabola by using equation 4-33.

Note: The step-by-step procedure is outlined, and Figure 4-13 is drawn, as if there is an intersection between the initial straight-line portion of the *p-y* curve and the parabolic portion of the curve at point k. However, in some instances there may be no intersection with the parabola. Equation 4-32 defines the *p-y* curve until there is an intersection with another branch of the *p-y* curve or if no intersection occurs, equation 4-32 defines the complete *p-y* curve. The soil-response curves for other depths can be found repeating the above steps for each desired depth.

(4) Recommended soil tests. Triaxial compression tests are recommended for obtaining the angle of internal friction of the sand. Confining pressures should be used which are close or equal to those at the depths being considered in the analysis. Tests must be performed to determine the unit weight of the sand. In many instances, however, undisturbed samples of sand cannot be obtained and the value of ϕ must be obtained from correlations with static cone penetration tests or from dynamic penetration tests (Table 4-4).

4. Analytical Method

The solution of the problem of the pile under lateral load must satisfy two general conditions. The equations of equilibrium must be solved and deflections and deformations must be consistent and compatible. These two requirements are fulfilled by finding a solution to the following differential equation (Hetenyi 1946).

$$EI\frac{d^4y}{dx^4} + P_x\frac{d^2y}{dx^2} - p - W = 0 \qquad (4\text{-}38)$$

where

P_x = axial load on the pile

y = lateral deflection of the pile at a point x along the length of the pile

p = soil reaction per unit length

EI = flexural rigidity

W = distributed load along the length of the pile

Other beam formulae which are useful in the analysis are:

$$EI\frac{d^3y}{dx^3} = V \qquad (4\text{-}39)$$

Table 4-5
Representative Values of *k* (lb/cu in.) for Sand

	Relative Density		
	below 35%	**35% to 65%**	**above 65%**
Recommended *k* for sand below water table	20	60	125
Recommended *k* for sand above water table	25	90	225

$$EI\ \frac{d^2y}{dx^2} = M \tag{4-40}$$

and

$$\frac{dy}{dx} = S \tag{4-41}$$

where

V = shear at point x along the length of the pile

M = bending moment of the pile

S = slope of the elastic curve

Solutions of the above equations can be made by use of the computer program described in this chapter. Nondimensional methods, described later, can frequently be used to obtain acceptable solutions but those methods are much less versatile than the computer method. An acceptable technique for getting solutions to the equations governing the behavior of a laterally loaded pile is to formulate the differential equation in difference terms. The pile is divided into n increments of constant length h. Equation 4-38 can be represented at point m along the pile as follows:

$$\begin{aligned} y_m - 2^R m - 1 &+ y_{m-1}\,(-2R_{m-1} - 2Rm \\ &+ P_x h^2) + y_m(R_{m-1} + 4R_m \\ &+ R_{m+1} - 2P_x h^2 + k_m h^4) \\ &+ y_{m+1}(-2R_m - 2R_m + 1 \\ &+ P_x h^2) + y_{m+2} R_m + 1 - W_m = 0 \end{aligned} \tag{4-42}$$

where

y_m = deflection at point m

R_m $E_m I_m$ = flexural rigidity at point m

P_x = axial load (causes no moment at $x = 0$)

k_m = $\frac{p_m}{y_m}$ = soil modulus at point m

W_m = distributed load at point m

Because the pile is divided into n increments, there are $n + 1$ points on the pile and $n + 1$ of the above equations can be written. The differential equation in difference form uses deflections at two points above and at two points below the point being considered. Therefore, four imaginary deflections are introduced, two at the top of the pile and two at the bottom. The introduction of four boundary conditions, two at the bottom of the pile and two at the top, yields $n + 5$ simultaneous equations of a sort to be easily and quickly solved by the digital computer. After solving the simultaneous equations, shear moment and slope can be found at all points along the pile by solving equations 4-39, 4-40, and 4-41. The soil resistance p can be found to be the product $k_m y_m$. It is obvious that an iterative solution must be made with the computer because the values of the soil moduli k_m are not known at the outset. Convergence to the correct solution is judged to have been achieved when the difference between the final two sets of computed deflections are less than the value of the tolerance selected by the engineer.

a. Boundary conditions. At the bottom of the pile the two boundary conditions employed are the shear and the moment, and both are equal to zero. Thus, a solution can be obtained for a short pile such that there is a significant amount of deflection and slope at the bottom of the pile.

Sometimes the question arises about the possibility of forces at the base of the pile due to development of shearing stresses from the soil when the bottom of the file is deflected. That possibility can readily be accommodated by placing a *p-y* curve with appropriate numerical values at the bottom increment of the pile. There are three boundary conditions to be selected at the top of the pile, but one of those, the axial load, provides no specific information on pile-head deflection. Thus, two other boundary conditions must be selected. The computer is programmed to accept one of the following three sets. (The axial load is assumed to be used with each of these sets).

(1) The lateral load (P_t) and the moment (M_t) at the top of the pile are known.

(2) The lateral load (P_t) and the slope of the elastic curve (S_t) at the top of the pile are known.

(3) The lateral load (P_t) and the rotational-restraint constant (M_t/S_t) at the top of the pile are known.

The first set of boundary conditions applies to a case such as a highway sign where wind pressure applies a force some distance above the groundline. The axial load will usually be small and a free body of the pile can be taken at the groundline where the shear and the moment will be known. The second set of boundary conditions can be employed if a pile supports a retaining wall or bridge abutment and where the top of the pile penetrates some distance into a reinforced concrete mat. The shear will be known, and the pile-head rotation in most cases can be assumed to be zero. The third set of boundary conditions is encountered when a pile frames into a superstructure that is flexible. In some bridge structures, the piles could continue and form the lower portion of a column. A free body of the pile can be taken at a convenient point, and the rotational restraint (M_t/S_t) of the portion of the structure above the pile head can be estimated. The magnitude of the shear will be known. Iteration between pile and superstructure will lead to improved values of rotational restraint and convergence to an appropriate solution can be achieved.

b. U.S. Army Engineer Waterways Experiment Station (WES) computer program COM624G (IOO12). The method for solving the governing equations for the single pile under lateral loading and the recommendations for *p-y* curves have been incorporated into a computer program that is available from WES. The user is urged to read the documentation that accompanies the computer diskettes and to solve the examples that are included. Users are assumed to be engineers who can understand the importance of verifying the accuracy of any given solution. Solutions are obtained rapidly to allow the user to investigate the importance and influence of various parameters. For example, upper-bound and lower-bound values of the soil properties can be input and the outputs compared. This exercise will give the user an excellent idea of the possible variation of behavior across a site and may indicate the desirability of performing a full-scale field test.

c. Nondimensional method of analysis.

(1) Variation of soil modulus with depth. Prior to presenting the details of nondimensional analysis, it is desirable to discuss the nature of the soil modulus. A pile under lateral loading is shown in Figure 4-16a and a set of *p-y* curves is shown in Figure 4-16b. As shown in the figure, the ultimate value of *p* and the initial slope of the curves increase with depth, as is to be expected in many practical cases. Also shown in Figure 4-16b is the possible deflected shape of the pile under load and the secants to the point on the curves defined to be the respective deflection. The values of soil modulus E_s so obtained are plotted as a function of depth in Figure 4-16c. The line passing through the plotted points defines the variation of E_s with depth. In the case depicted in Figure 4-16, the following equation defines the variation in the soil modulus.

$$E_s = kx \tag{4-43}$$

It is of interest to note that neither E_s nor k are constants, but each of them decrease as the load and deflection increase. In many cases encountered in practice, the value E_s would not be zero at the groundline and would not increase linearly with depth, as shown in Figure 4-16. However, these are two things that suggest that equation 4-43 will frequently define, at least approximately, the variation of the soil modulus with depth. First, the soil strength and stiffness will usually increase with depth. Second, the pile deflection will always be larger at and near the groundline. Furthermore, experience with nondimensional solutions has shown that it is not necessary to pass a curve precisely through the soil-modulus values, as is done by the computer, to obtain an acceptable solution.

(2) Nondimensional equations and curves. The derivation of the equations for the nondimensional solutions are not shown here but may be seen in detail elsewhere (Reese and Matlock 1956; Matlock and Reese 1961). The following sections present the equations and nondimensional curves for three cases: pile head free to rotate, pile head fixed against rotation, and pile head restrained against rotation. The nondimensional solutions are valid only for piles that have constant stiffness *EI* and no with axial load. These restrictions are not very important in many cases because computer solutions usually show that deflections and bending moments are only moderately influenced by changes in *EI* and by the presence of an axial load. Also, the principal benefits from the nondimensional method are in

checking computer solutions and in allowing an engineer to gain insight into the nature of the problem; thus, precision is not required. As may be seen by examining published derivations (Matlock and Reese 1961), nondimensional curves can be developed for virtually any conceivable variation in soil modulus with depth. However, studies show (Reese 1984) that the utility of some more complex forms of variation ($E_s = k_1 + k_2x, E_s = kx^n$) is limited when compared to the simpler form ($E_s = kx$).

d. Pile head free to rotate (Case I). The procedure shown in this section may be used when the shear and moment are known at the groundline. A single pile that serves as the foundation for an overhead sign, such as those that cross a highway, is an example of the Case I category. The shear and moment at the groundline may also be known, or computed, for some structural configurations for bridges.

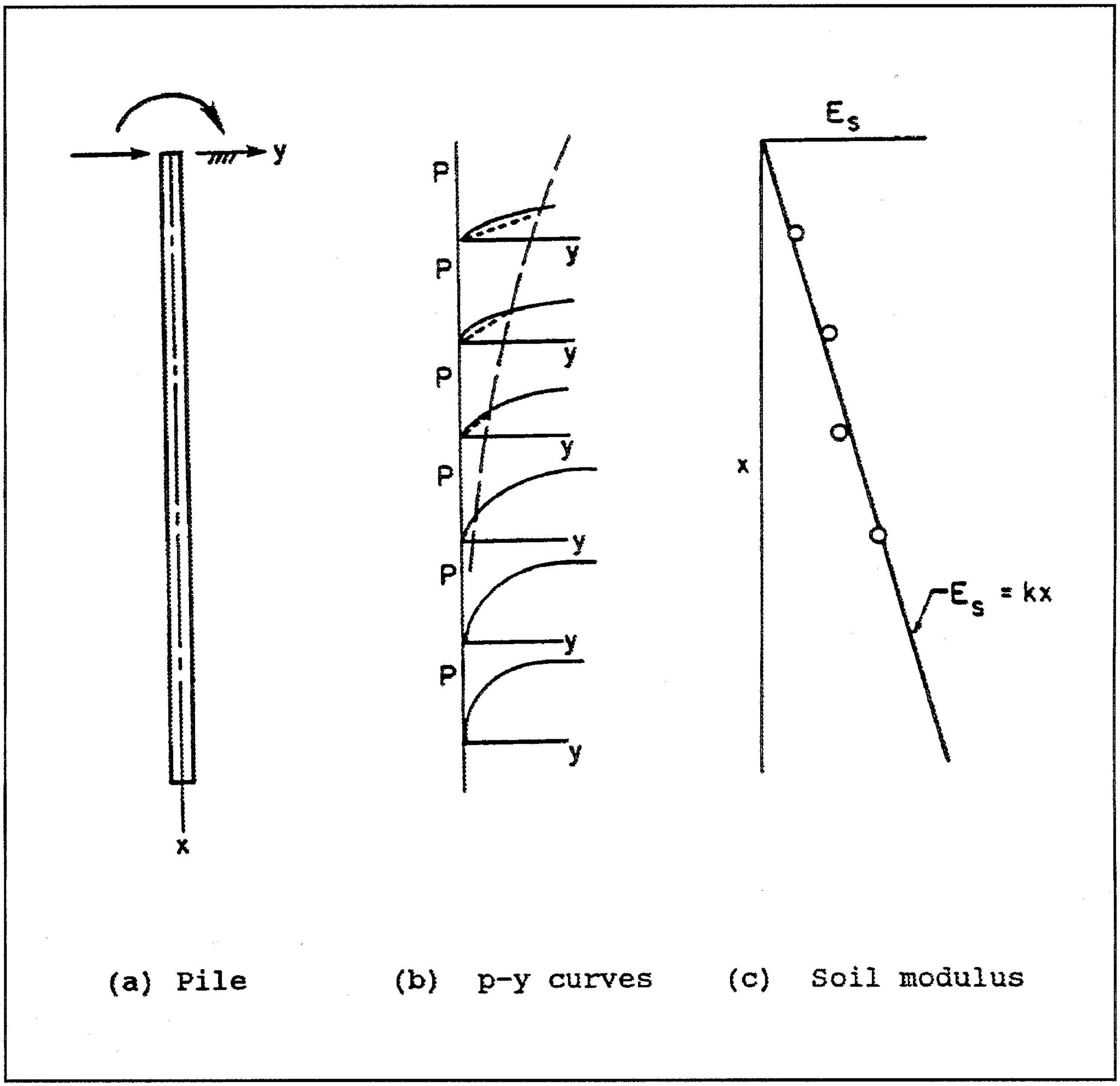

Figure 4-16. Form of variation of soil modulus with depth

(1) Construct p-y curves at various depths by procedures recommended herein, with the spacing between p-y curves being closer near the ground surface than near the bottom of the pile.

(2) Assume a convenient value of a relative stiffness factor T, perhaps 100 inches. The relationship is given as:

$$T = \left(\frac{EI}{k}\right)^{1/5} \tag{4-44}$$

where

EI = flexural rigidity of pile

k = constant relating the secant modulus of soil and reaction of depth ($E_s = kx$)

(3) Compute the depth coefficient z_{max}, as follows:

$$z_{max} = \frac{x_{max}}{T} \tag{4-45}$$

where x_{max} equals the embedded length of the pile.

(4) Compute the deflection y at each depth along the pile where a p-y curve is available by using the following equation:

$$y = A_y \frac{P_t T^3}{EI} + B_y \frac{M_t T^2}{EI} \tag{4-46}$$

where

A_y = deflection coefficient, found in Figure 4-17

P_t = shear at top of pile

T = relative stiffness factor

B_y = deflection coefficient, found in Figure 4-18

M_t = moment at top of pile

EI = flexural rigidity of pile

The particular curves to be employed in getting the A_y and B_y coefficients depend on the value of z_{max} computed in step 3. The argument for entering Figures 4-17 and 4-18 is the nondimensional depth z, where z is equal to x/T.

(5) From a p-y curve, select the value of soil resistance p that corresponds to the pile deflection value y at the depth of the p-y curve. Repeat this procedure for every p-y curves that is available.

(6) Compute a secant modulus of soil reaction E_s ($E_s = -p/y$). Plot the E_s values versus depth (see Figure 4-16c).

(7) From the E_s versus depth plotted in step 6, compute the constant k which relates E_s to depth ($k = E_s/x$). Give more weight to E_s values near the ground surface.

(8) Compute a value of the relative stiffness factor T from the value of k found in step 7. Compare this value of T to the value of T assumed in step 2. Repeat steps 2 through 8 using the new value of T each time until the assumed value of T equals the calculated value of T.

(9) When the iterative procedure has been completed, the values of deflection along the pile are known from step 4 of the final iteration. Values of soil reaction may be computed from the basic expression: $p = E_s y$. Values of slope, moment, and shear along the pile can be found by using the following equations:

$$S = A_s \frac{P_t T^2}{EI} + B_s \frac{M_t T}{EI} \tag{4-47}$$

$$M = A_m P_t T + B_m M_t \tag{4-48}$$

$$V = A_v P_t + B_v \frac{M_t}{T} \tag{4-49}$$

The appropriate coefficients to be used in the above equations may be obtained from Figures 4-19 through 4-24.

e. Pile head fixed against rotation (Case II). The method shown here may be used to obtain solution for the case where the superstructure translates under load but does not rotate and where the superstructure is very, very stiff in relation to the pile. An example of such a case is where the top of a pile is embedded in a reinforced concrete mat as for a retaining wall or bridge abutment.

(1) Perform steps 1, 2, and 3 of the solution procedure for free-head piles, Case I.

(2) Compute the deflection y_F at each along the pile where a p-y curve is available by using the following equation:

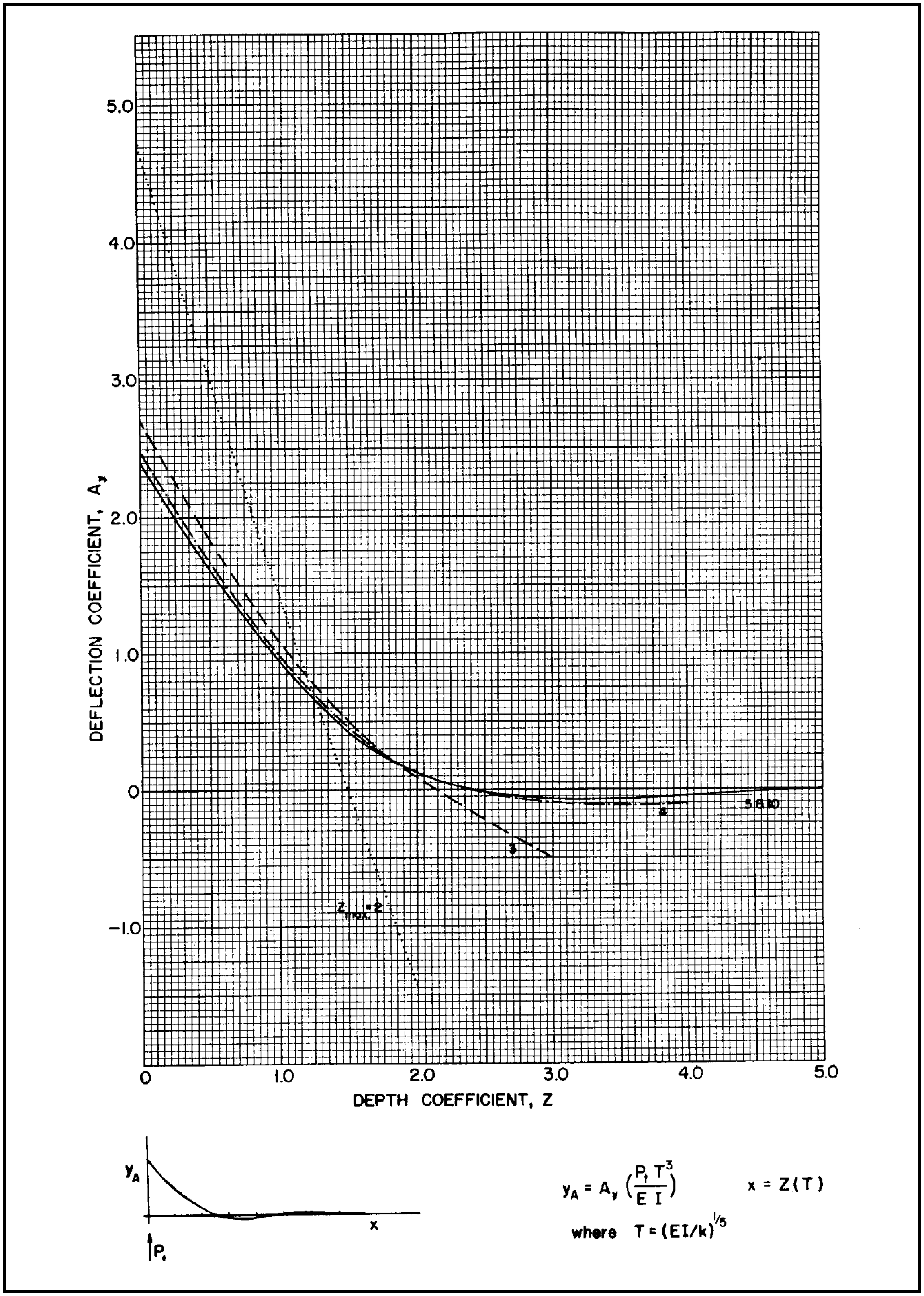

Figure 4-17. Pile deflection produced by lateral load at mudline

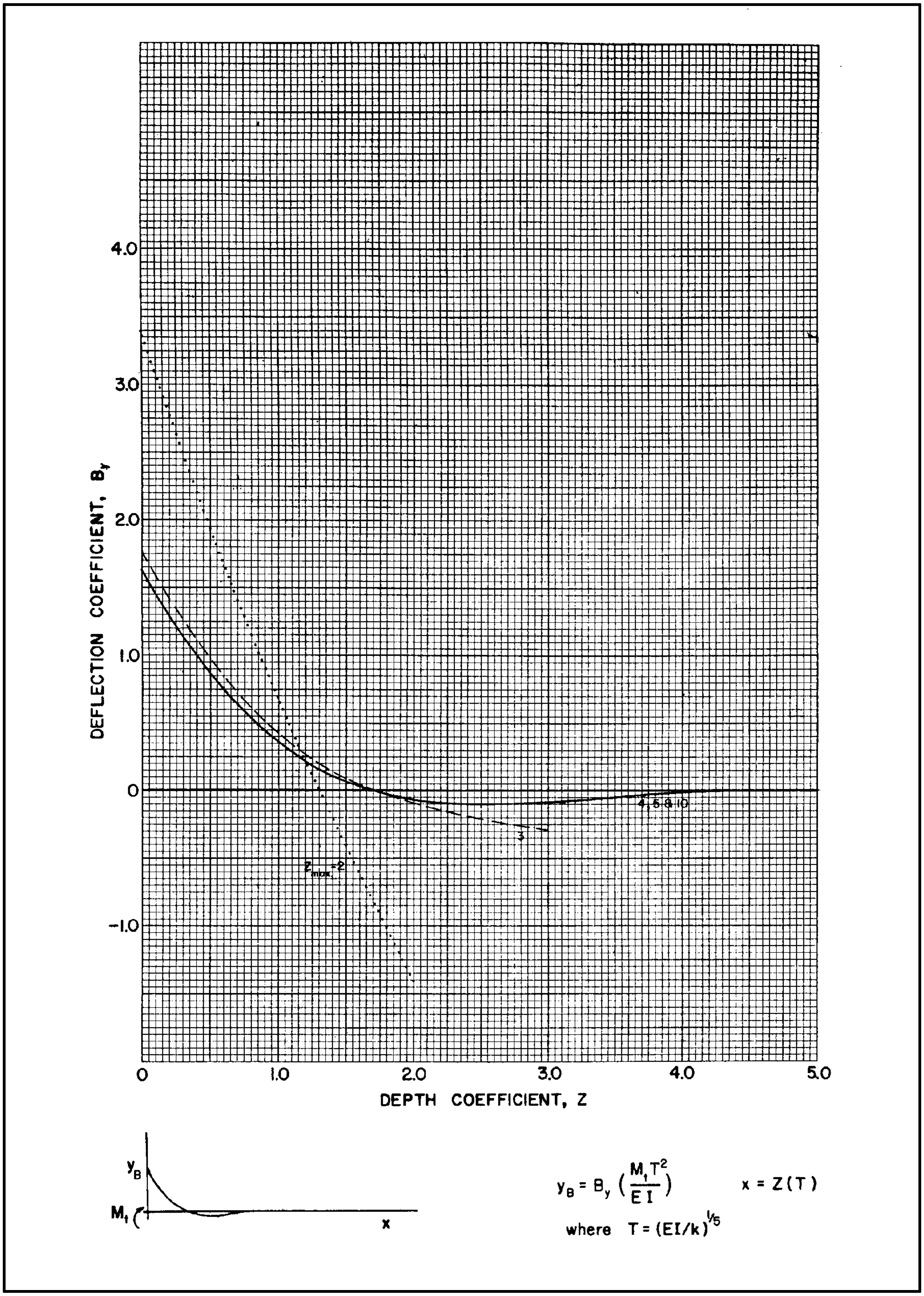

Figure 4-18. Pile deflection produced by moment applied at mudline

$$y_F = F_y \frac{P_t T^3}{EI} \qquad (4\text{-}50)$$

The deflection coefficients F_y may be found by entering Figure 4-25 with the appropriate value of z_{max}.

(3) The solution proceeds in steps similar to those of steps 5 through 8 for the free-head case.

(4) Compute the moment at the top of the pile M_t from the following equation:

$$M_t = F_{Mt} P_t T \qquad (4\text{-}51)$$

The value of F_{Mt} may be found by entering Table 4-6 with the appropriate value of z_{max}, where z_{max} is the maximum depth coefficient.

Table 4-6
Moment Coefficients at Top of Pile for Fixed-Head Case

z_{max}	F_M
2	-1.06
3	-0.97
4	-0.93
5 and above	-0.93

(5) Compute the values of slope, moment, shear, and soil reaction along the pile by following the procedure in step 9 for the free-head pile.

f. Pile head restrained against rotation (Case III). Case III may be used to obtain a solution for the case where the superstructure translates under load, but rotation at the top of the pile is partially restrained. An example of Case III is when the pile is extended and becomes a beam-column of the superstructure. A moment applied to the bottom of the beam-column will result in a rotation, with the moment-rotation relationship being constant. That relationship, then, becomes one of the boundary conditions at the top of the pile.

(1) Perform steps 1, 2, 3 of the solution procedures for free-head piles, Case I.

(2) Obtain the value of the spring stiffness k_θ of the pile superstructure system. The spring stiffness is defined as follows:

$$k_\theta = \frac{M_t}{S_t} \qquad (4\text{-}52)$$

where

M_t = moment at top of pile

S_t = slope at top of pile

(3) Compute the slope at the top of pile S_t as follows:

$$S_t = A_{st} \frac{P_t T^2}{EI} + B_{st} \frac{M_t T}{EI} \qquad (4\text{-}53)$$

where

A_{st} = slope coefficient at $z = 0$, found in Figure 4-19

B_{st} = slope coefficient at $z = 0$, found in Figure 4-20

(4) Solve equations 4-52 and 4-53 for the moment at the top of the pile M_t.

(5) Perform steps 4 through 9 of the solution procedure for free-head piles, Case I.

g. Solution of example problem. To illustrate the solution procedures, an example problem is presented. The example will be solved principally by the nondimensional method. The solution, while somewhat cumbersome, yields an excellent result in the case selected. The nondimensional method has several advantages: (1) the elements of a solution are clearly indicated; (2) the method is useful for practical cases if a computer and the necessary software are unavailable; and (3) the method is capable of providing a check to the output of the computer.

(1) Select pile dimensions and calculate ultimate bending moment (step 1). The pile is an HP 12 by 84 with the load applied perpendicular to the major axis. The width is 12.295 inches and the depth is 12.28 inches. The moment of inertia about the major axis is 650 in.^{4}, the cross-sectional area is 24.6 square inches, and the ultimate bending moment is 4,320 inch-kips, assuming a yield strength of the steel of 36 kips per square inch ignoring the effect of axial load. The length, penetration below the ground surface, is assumed to be 80 feet.

(2) Study soil profile and idealize soil as clay with $\phi = 0$ or as sand with $c = 0$ (step 2). This step would normally require the evaluation of the results of field exploration and

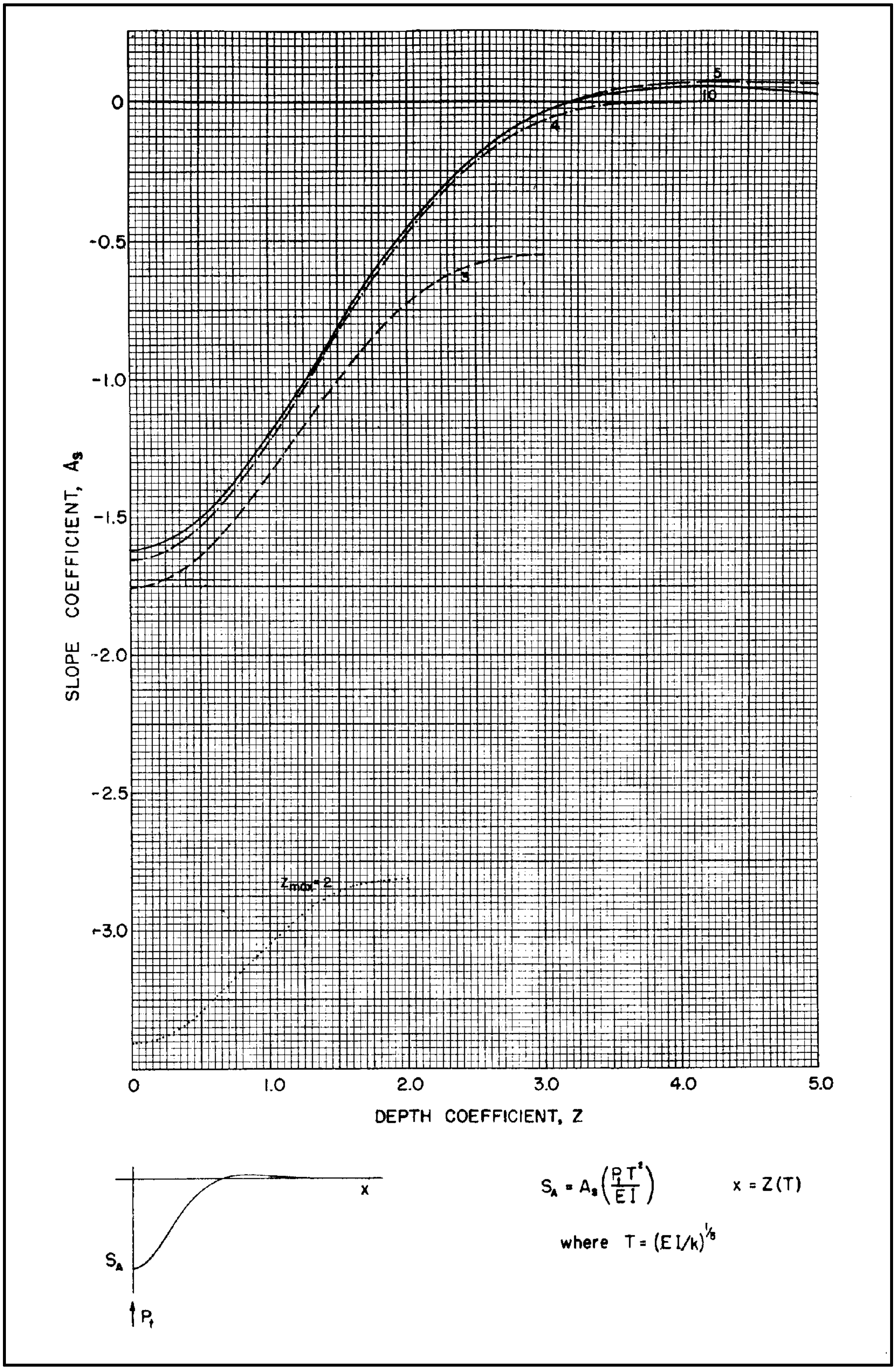

Figure 4-19. Slope of pile caused by lateral load at mudline

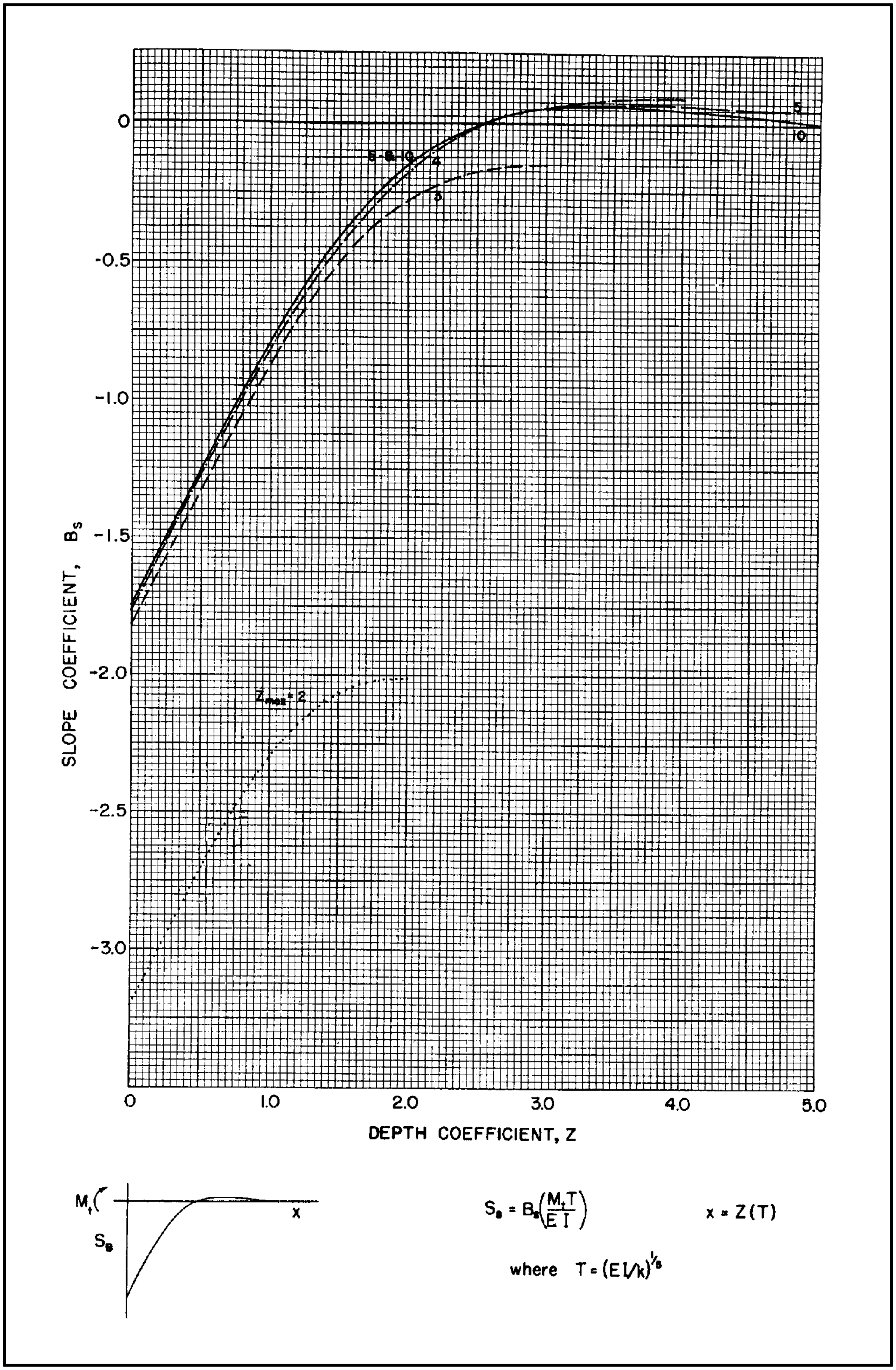

Figure 4-20. Slope of pile caused by moment applied at mudline

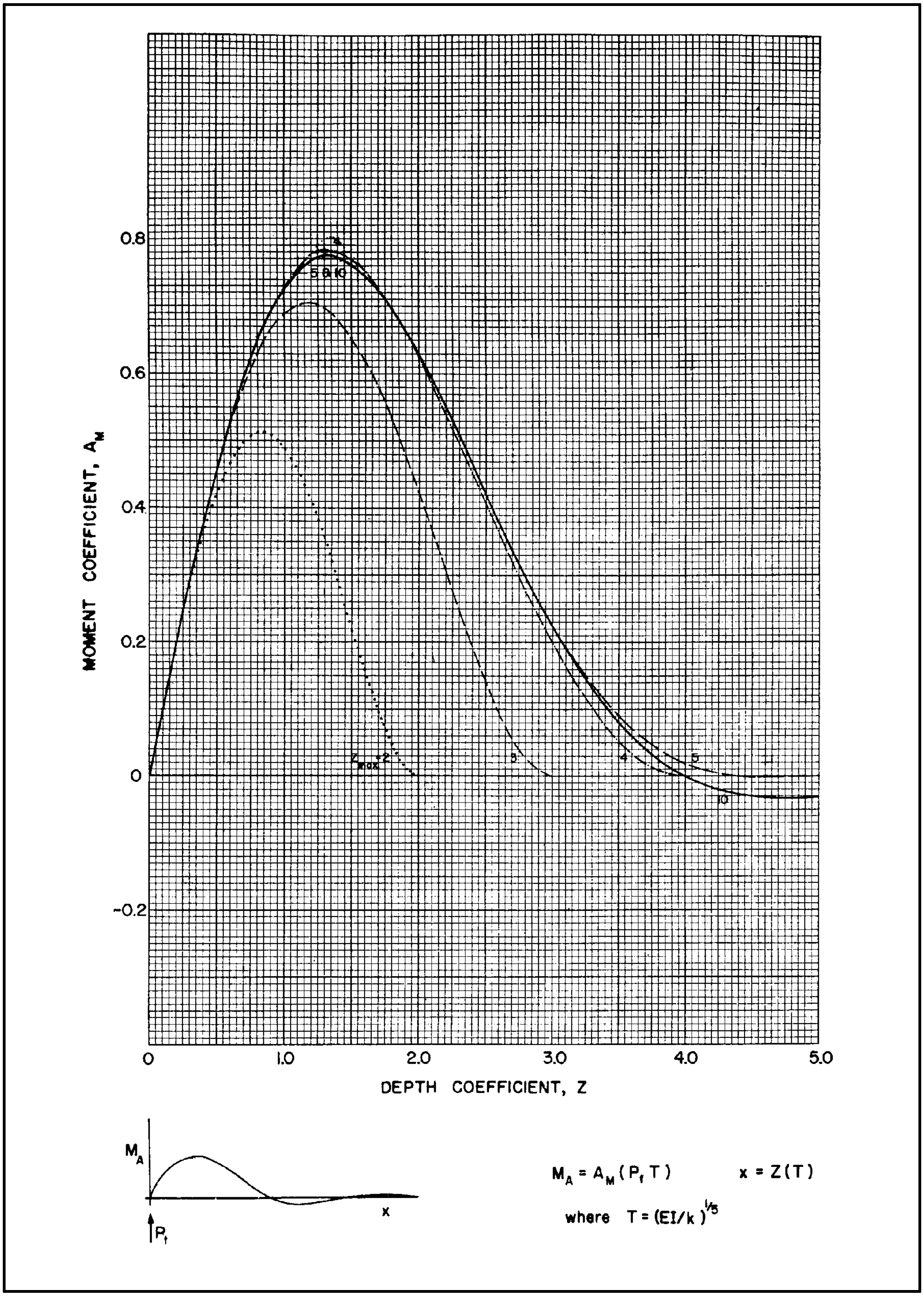

Figure 4-21. Bending moment produced by lateral load at mudline

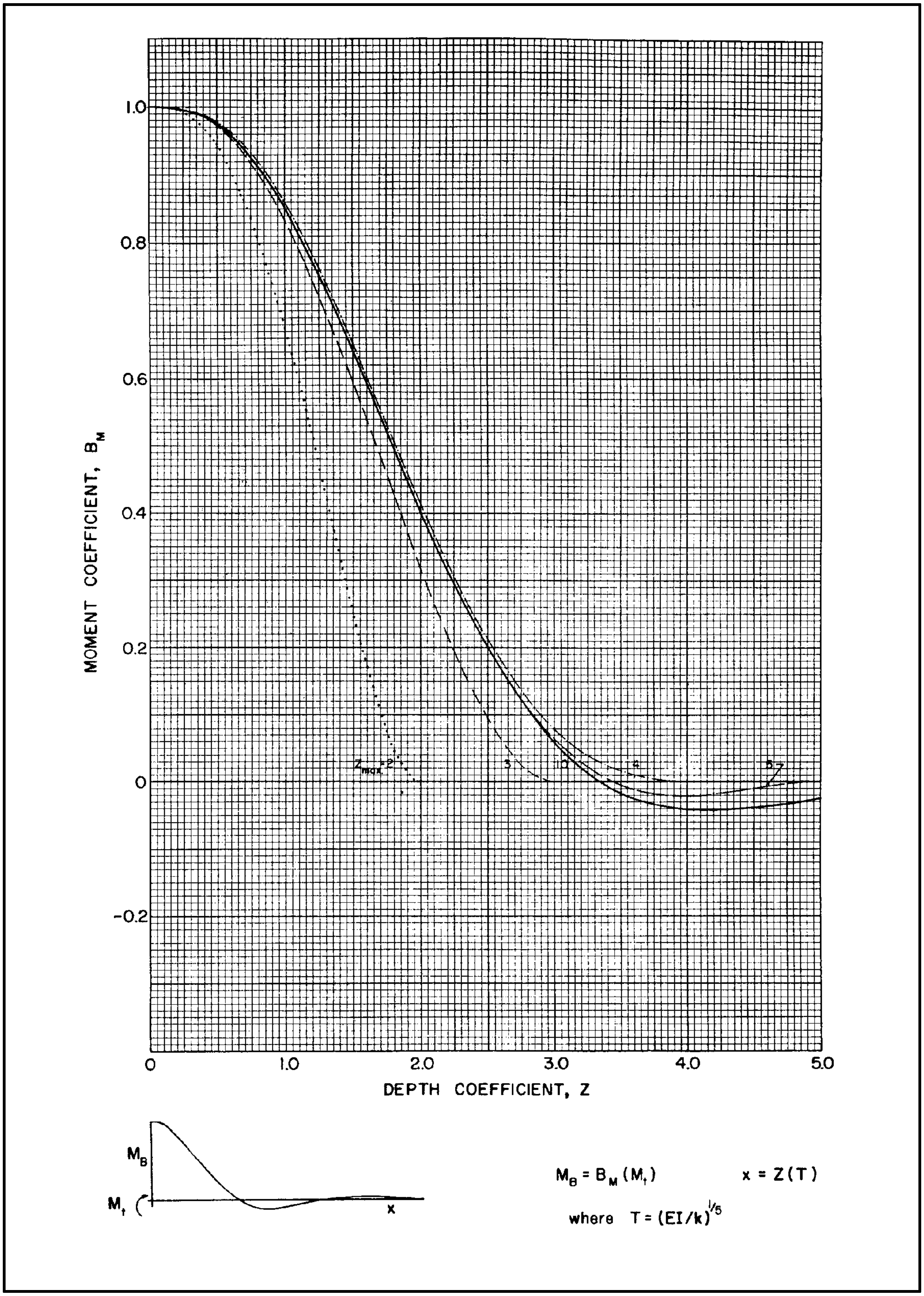

Figure 4-22. Bending moment produced by moment applied at mudline

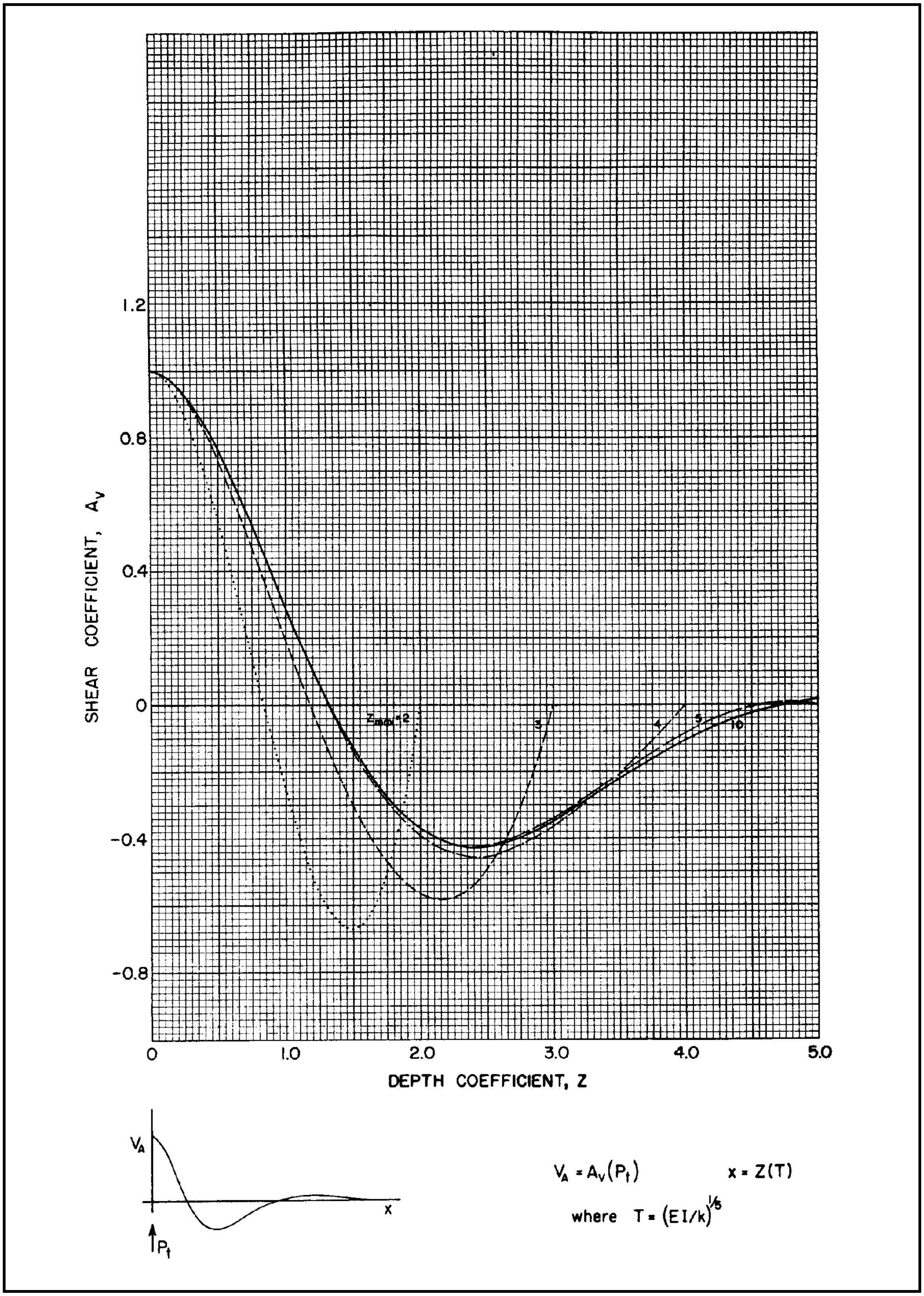

Figure 4-23. Shear produced by lateral load at mudline

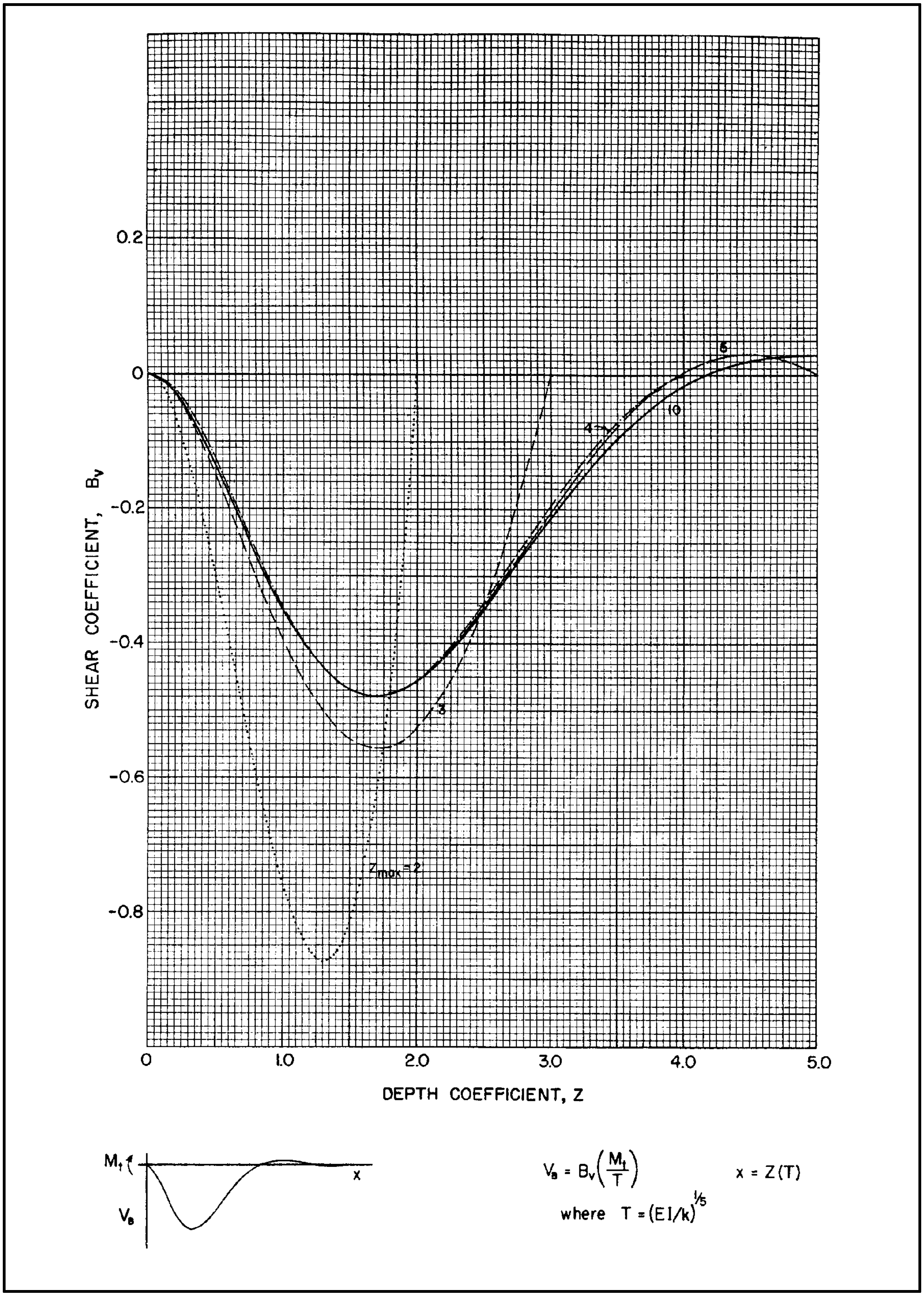

Figure 4-24. Shear produced by moment applied at mudline

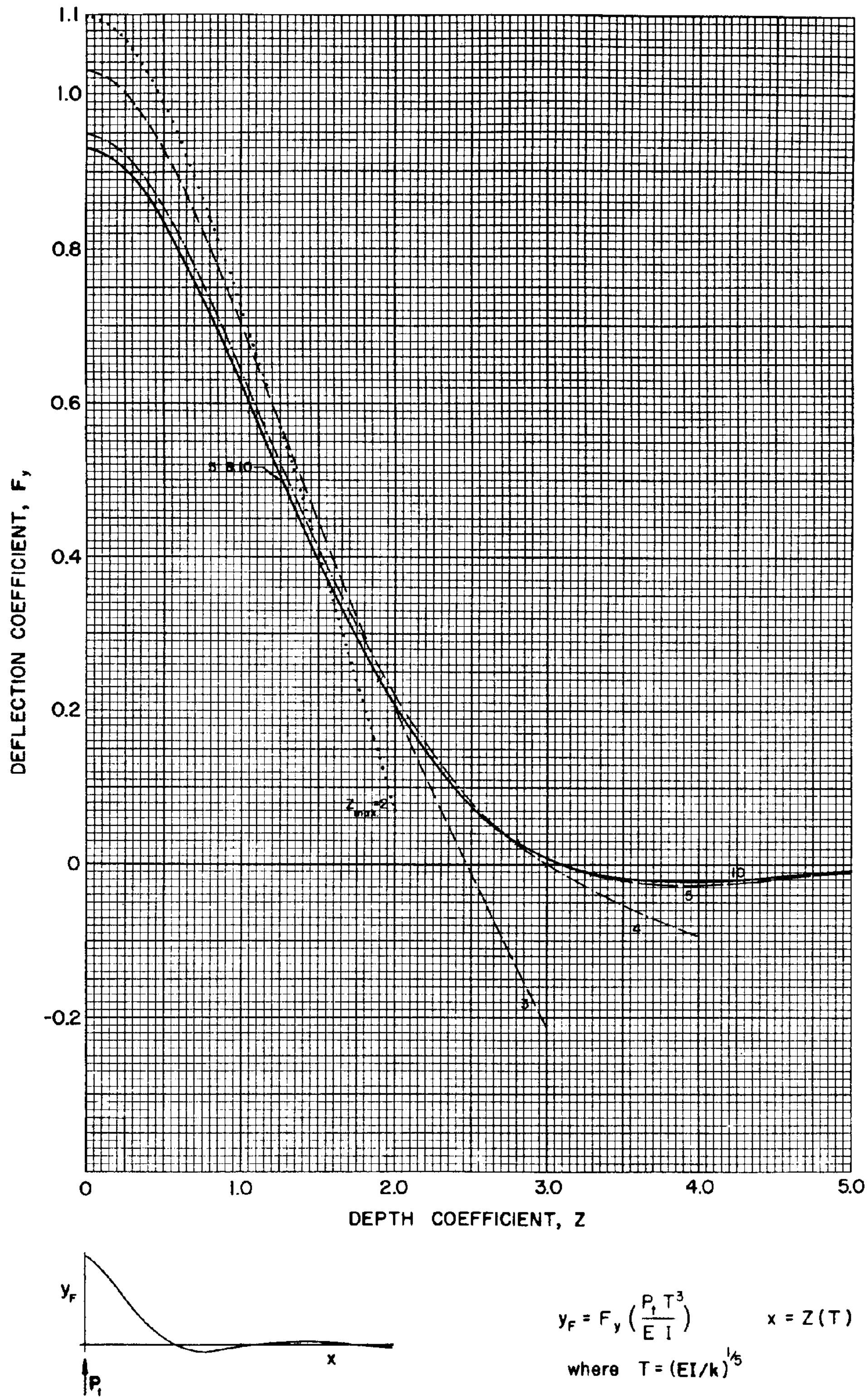

Figure 4-25. Deflection of pile fixed against rotation at mudline

laboratory testing, but for the example problem the soil is assumed to be a sand with an angle of internal friction of 35 degrees and with the water table at the ground surface. The submerged unit weight of the soil is assumed to be 0.04 pounds per cubic inch.

(3) Study soil-response (*p-y*) curves (step 3). The procedures described earlier for sand were used and the *p-y* curves were developed. For the structural shape, the diameter of the pile was selected as equal to the width. The curves are presented in Figure 4-26. The curves are spaced closer near the top of the pile where deflection is the largest. If the computer is employed, this step is unnecessary because the subroutines for the responses of the soil are implemented in the program. However, the user may have *p-y* curves produced for examination, if desired. For the hand solution, demonstrated herein, the *p-y* curves are shown in Figure 4-26. For the curve of the ground surface, zero depth, the *p*-values are zero for all values of *y*. The nonlinearity in the curves is evident, but it is of interest to note that there is no deflection-softening for the sand.

(4) Select set of loads and boundary conditions (step 4). If the computer program, COM624G, is being used, the engineer may select a set of loads and input the set into the program. Only a minimum set of output could be specified for each load; for example, pile-head deflection and maximum bending moment. The boundary conditions at the pile head can also be varied during these computations. The computer will rapidly produce the results, and the engineer may monitor the results on the screen and select another set for more complete output by hard copy and/or graphics. The deflection and bending moment, and other values, will be produced for points along the pile. In any case, the plan should be to find the loading that will generate the maximum bending moment or the maximum allowable deflection. A global factor of safety can be used and the results obtained for the case of the working load. All of the computations could be by the hand solution except that the axial loading cannot be included as affecting the lateral deflection and except that the pile cannot be shown as having different stiffnesses with depth. In any case, the hand solutions will be very time-consuming. However, to indicate the analytical process, a lateral load P_t of 30 kips was selected and the pile head was assumed to be free to rotate. This case might be similar to one of the piles that support a lock and dam, where the pile head extends only a short distance into the concrete base.

(5) Solve for deflection and bending moment (step 5). The first part of this step is to use the method for a hand solution and to solve for the response of the pile to the loading and boundary condition shown above. There is little information to be used in the selection of the initial value of the relative stiffness factor *T*, so a convenient value is selected. It is noted that the computations are with units of pounds and inches, for convenience.

(a) Trial 1

L = 80 ft (960 in.)

T = 100 in.

= L/T

z_{max} = 960/100 = 9.6; use curves for a "long" pile

$$y = A_y \frac{P_t T^3}{EI} = A_y \frac{(30{,}000)\ (100)^3}{(29{,}000{,}000)\ (650)}$$
$$= 1.592\ A_y$$

The computational table should be set up to correspond to the depths of the *p-y* curves.

The values of E_s are plotted in Figure 4-27a as a function of *x* with the result for *k* as shown below.

$$k = 270/100 = 2.70\ \text{lb/in.}^3$$

The value of the relative stiffness factor *T* that was obtained can now be found.

$$T = \sqrt[5]{\frac{EI}{K}}\ \sqrt[5]{\frac{(29 \times 10^6)\ (650\ \text{in.}^4)}{2.70}}$$
$$= 93.1\ \text{inches}$$

The value of *T* that was obtained is lower than the one that was tried. The second trial needs to use a still lower value to help to achieve a convergence.

(b) Trial 2

T = 50 inches

z_{max} = 960/50 = 19.2; use curves for a "long" pile

$$y = A_y \frac{P_t T^3}{EI} = A_y \frac{(30{,}000)\ (50)^3}{(29{,}000{,}000)\ (650)}$$
$$= 0.1989\ A_y$$

The values of E_s are plotted in Figure 4-27a as a function of *x* with the result for *k* as shown below.

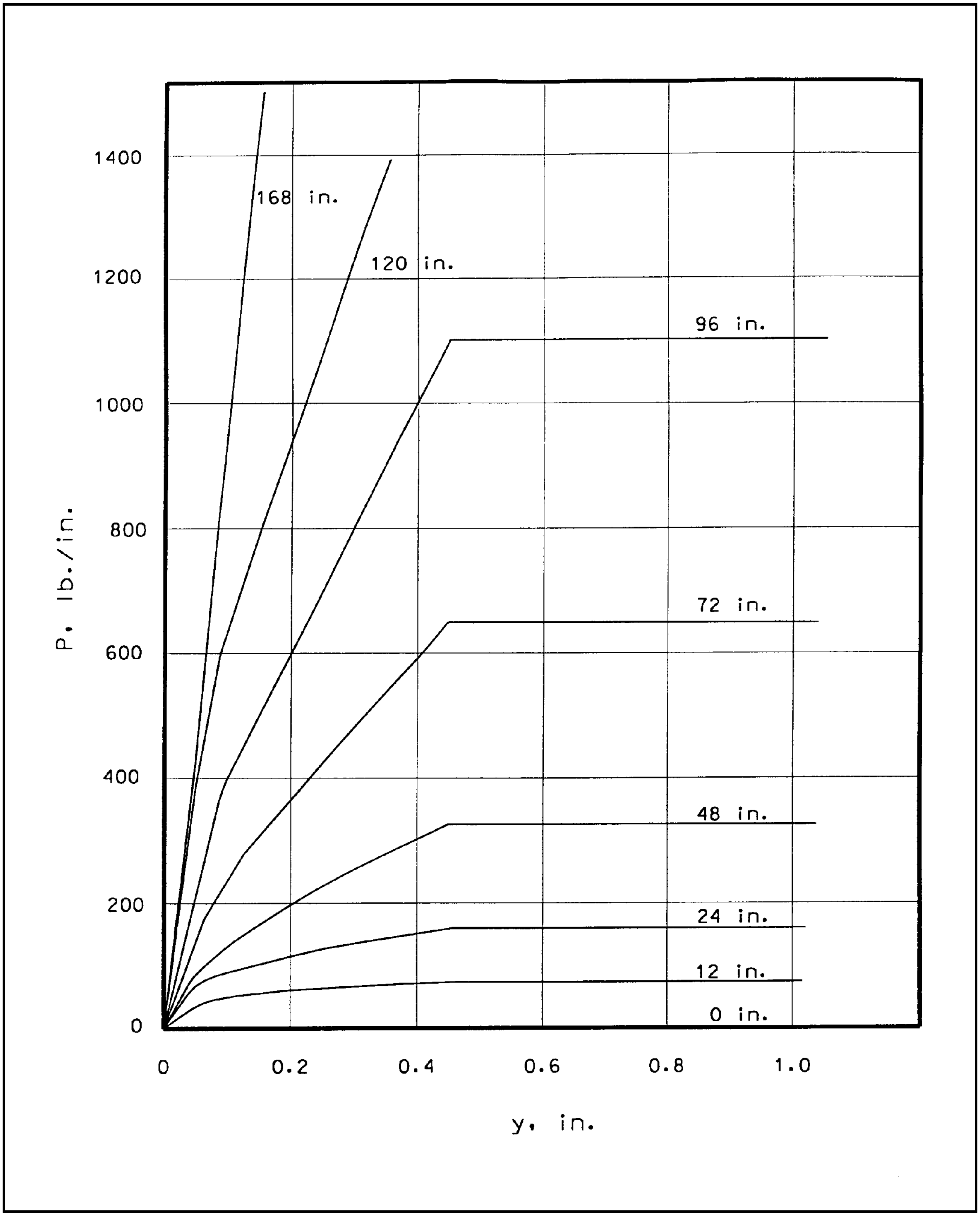

Figure 4-26. Soil-response curves

Depth (in.)	$z = x/t$	A_y	Deflection (in.)	Soil Resistance (lb/in.)	E_s (lb/sq in.)
0	0.00	2.4	3.82	0	0
12	0.12	2.25	3.58	77	22
24	0.24	2.0	3.18	165	52
48	0.48	1.7	2.71	320	118
72	0.72	1.3	2.07	625	302
96	0.96	1.0	1.59	1,125	708
120	1.2	0.75	1.19	---	---
168	1.68	0.2	0.32	---	---

Depth (in.)	$z = x/t$	A_y	Deflection (in.)	Soil Resistance (lb/in.)	E_s (lb/sq in.)
0	0.00	2.4	0.477	0	0
12	0.24	2.0	0.398	75	188
24	0.48	1.7	0.338	135	399
48	0.96	1.0	0.199	185	930
72	1.44	0.5	0.100	225	2,250
96	1.92	0.15	0.030	---	---
120	2.40	0.00	0.000	---	---
168	3.32	---	---	---	---

$$k = 1{,}000/47 = 21.28 \text{ lb/in.}^3$$

The value of the relative stiffness factor T that was obtained can now be found.

$$T = \sqrt[5]{\frac{EI}{K}} \sqrt[5]{\frac{(29 \times 10^6)\ (650 \text{ in.}^4)}{21.28}}$$

$$= 61.6 \text{ inches}$$

The values of T obtained are plotted versus T tried in Figure 4-27b. The converged value for T is approximately 84 inches. The reader may see that values for the A_y coefficients were obtained only approximately from the curve and that the values for the soil resistance corresponding to a computed deflection were obtained only approximately from the Figure giving the *p-y* curves. Also, there is no assurance that a straight line is correct between the plotted points for the two trials shown in Figure 4-27b. However, for the purposes of this demonstration no additional trials are made and the result is accepted as shown. The value of T of 84, a value of P_t of 30,000 pounds, and a value of EI of 18.85×10^9 lb-in.^{2} are employed in obtaining the curves of deflection and bending moment as a function of depth. The equations are shown below and the computations merely involve the selection of values from the nondimensional curves for the depths desired.

$$y = A_y \frac{P_t T^3}{EI} = A_y \frac{(30{,}000)\ (84)^3}{(29{,}000{,}000)\ (650)}$$

$$= 0.943\ A_y$$

$$M = A_m\ P_t\ T = 2.52 \times 10^6 \text{ in.-lb}$$

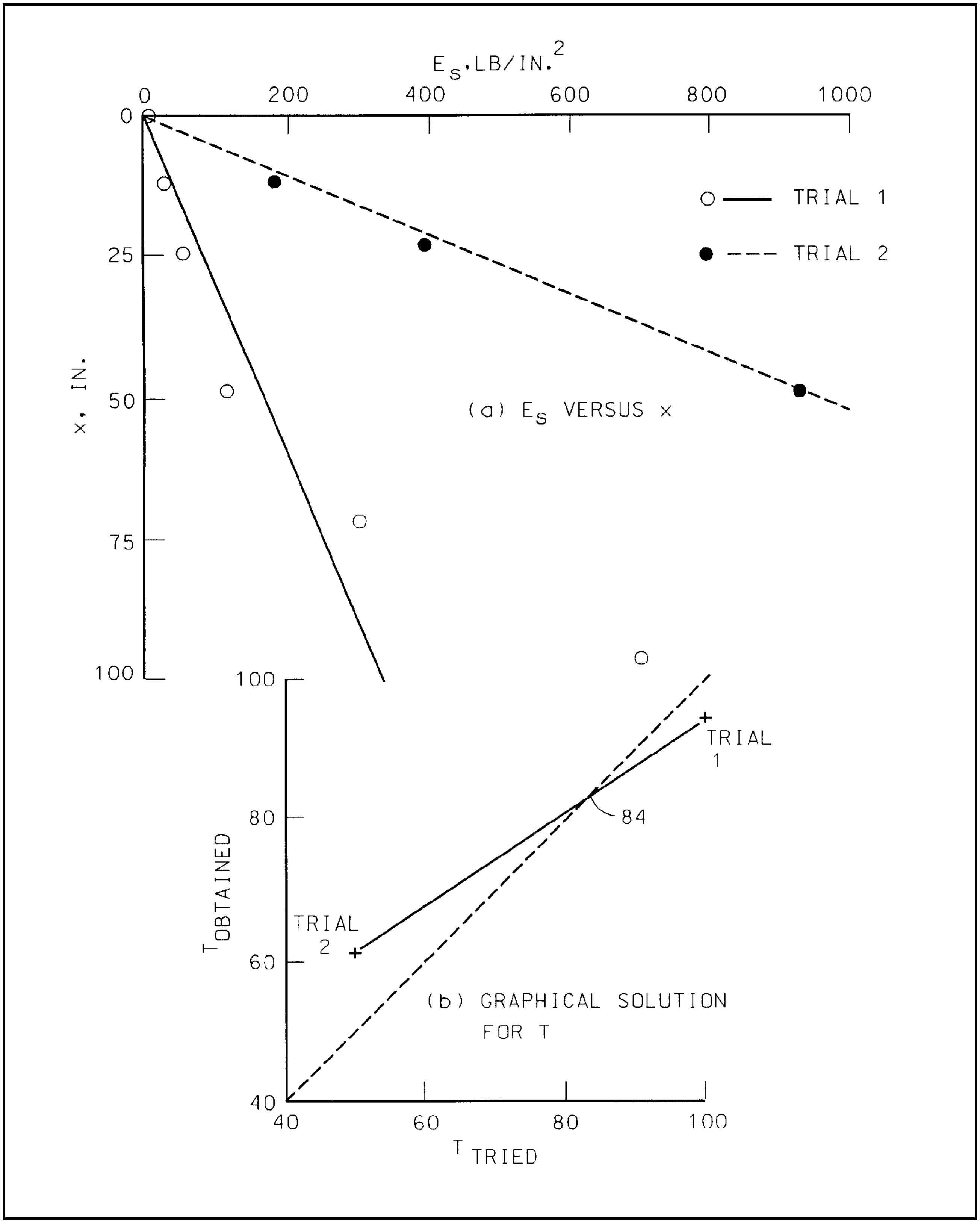

Figure 4-27. Graphical solution for relative stiffness factor

The following table shows the computation of the values of deflection and bending moment as a function of depth, using the above equations. The same problem was solved by computer and results from both methods are plotted in Figure 4-28. As may be seen, the shapes of both sets of curves are similar, the maximum moment from the hand method and from computer agree fairly well, but the computed deflection at the top of the pile is about one-half the value from the nondimensional method. One can conclude that a closed convergence may have yielded a smaller value of the relative stiffness factor to obtain a slightly better agreement between the two methods, but it is certain that the two methods could not have been brought into perfect agreement. An examination of Figure 4-27a shows that is impossible to fit a straight line through the plotted values of E_s versus depth; therefore, $E_s = kx$ will not yield a perfect solution to the problem, as demonstrated in Figure 4-28. However, even with imperfect fitting in Figure 4-27a and with the crude convergence shown in Figure 4-27b, the computed values of maximum bending moment from the hand solution and from computer agreed remarkably well. The effect of the axial loading on the deflection and bending moment was investigated with the computer by assuming that the pile had an axial load of 100 kips. The results showed that the groundline deflection increased about 0.036 inches, and the maximum bending moment increased about 0.058×10^6 in-lb; thus, the axial load caused an increase of only about 3 percent in the values computed with no axial load. However, the ability to use an axial load in the computations becomes important when a portion of a pile extends above the groundline. The computation of the buckling load can only be done properly with a computer code.

Depth (in.)	***z***	A_y	***y* (in.)**	A_M	***M* (in. lb/10^6)**
0	0.0	2.43	2.29	0.0	0
17	0.2	2.11	1.99	0.198	0.499
34	0.4	1.80	1.70	0.379	0.955
50	0.6	1.50	1.41	0.532	1.341
67	0.8	1.22	1.15	0.649	1.636
84	1.0	0.962	0.91	0.727	1.832
101	1.2	0.738	0.70	0.767	1.933
118	1.4	0.544	0.51	0.772	1.945
151	1.8	0.247	0.23	0.696	1.754
210	2.5	-0.020	-0.02	0.422	1.063
252	3.0	-0.075	-0.07	0.225	0.567
294	3.5	-0.074	-0.07	0.081	0.204
336	4.0	-0.050	-0.05	0.0	0

(6) Repeat solutions for loads to obtain failure moment (step 6). As shown in the statement about the dimensions of the pile, the ultimate bending moment was incremented to find the lateral load P_t that would develop that moment. The results, not shown here, yielded an ultimate load of 52 kips. The deflection corresponding to that load was about 3.2 inches.

(7) Apply global factor of safety (step 7). The selection of the factor of safety to be used in a particular design is a function of many parameters. In connection with a particular design, an excellent procedure is to perform computations with upper-bound and lower- bound values of the principal factors that affect a solution. A comparison of the results may suggest in a particular design that can be employed with safety. Alternatively, the difference in the results of such computations may suggest the performance of further tests of the soil or the performance of full-scale field tests at the

construction site.

5. Status of the Technology

The methods of analysis presented herein will be improved in time by the development of better methods of characterizing soil and by upgrading the computer code. In this latter case, the codes are being constantly refined to make them more versatile, applicable to a wider range of problems, and easier to use. From time to time tests are being performed in the field with instrumented piles. These tests, when properly interpreted, can lead to better ideas about the response of the soil. However, it is unlikely that there will be much changein the basic method of analysis. The solution of the difference equations by numerical techniques, employing curves at discrete locations along a pile to represent the response of the soil or distributed loading, is an effective method. The finite element method may come into more use in time but, at present, information on the characterization of the soil by that method is inadequate.

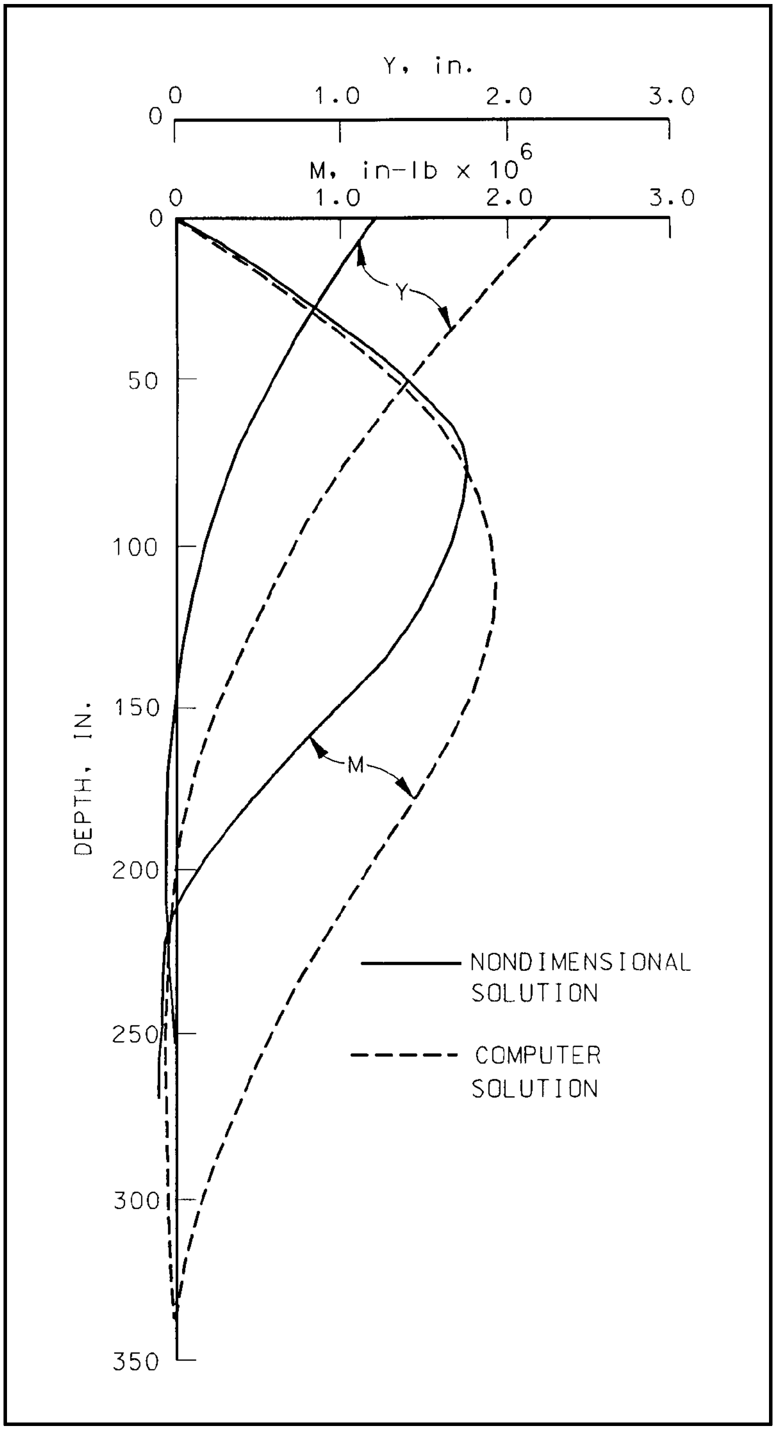

Figure 4-28. Comparison of deflection and bending moment from nondimensional and computer solutions